PHYSICAL REVIEW D **85,** 075024 (2012)

Analysis of the NMSSM Higgs boson masses at one-loop level

K. Ender,[1] T. Graf,[2] M. Mühlleitner,[1] and H. Rzehak[3,*]

[1]*Institut für Theoretische Physik, Karlsruhe Institute of Technology, 76128 Karlsruhe, Germany*
[2]*IPPP, Department of Physics, University of Durham, Durham DH1 3LE, UK*
[3]*CERN, Theory Division, 1211 Geneva 23, Switzerland*

(Received 12 December 2011; revised manuscript received 10 February 2012; published 26 April 2012)

For a reliable prediction of the NMSSM Higgs boson signatures at present and future high-energy colliders and a proper distinction of the NMSSM and MSSM Higgs sector the precise knowledge of the Higgs boson masses including higher-order corrections is indispensable. In this paper, the one-loop corrections to the neutral NMSSM Higgs boson masses and mixings are calculated in three different renormalization schemes. In addition to the $\overline{\text{DR}}$ renormalization scheme, existing in the literature, two other schemes are adopted. Furthermore, the dependence on the value of the top quark mass is investigated. From this and the variation of the renormalization scale, at one-loop level, the residual theory error due to missing higher-order corrections can be estimated to be of the order of 10%.

DOI: 10.1103/PhysRevD.85.075024 PACS numbers: 12.60.Jv

I. INTRODUCTION

Supersymmetric theories [1,2] provide a natural solution to the hierarchy problem [2,3]. The latter is related to the fact that the standard model (SM) Higgs boson mass receives radiative corrections which are quadratic in the cut-off scale, usually chosen to be the GUT scale $M_{\text{GUT}} = 10^{16}$ GeV. To keep the Higgs mass of the order of the electroweak (EW) scale an extreme fine-tuning of the model parameters is necessary. Supersymmetry (SUSY) introduces a new symmetry between fermionic and bosonic degrees of freedom, leading to extra contributions to the radiative corrections of the Higgs boson mass due to the new SUSY particles which cancel the dangerous quadratic divergence of their corresponding SM counterpart. In this way the Higgs mass is naturally kept at a phenomenologically valid level even in the presence of high mass scales.

As the superpotential must be analytic in the chiral superfields, two complex Higgs doublets have to be introduced, H_u to provide masses to the up-type fermions and H_d to ensure nonzero down-type fermion masses. In this way the theory is also kept anomaly-free. In the superpotential of the minimal supersymmetric extension of the standard model (MSSM) [4] the two Higgs doublet fields mix through the term $\mu H_u \epsilon H_d$ which involves the higgsino mass parameter μ. While the MSSM suffers from the μ problem [5], in the next-to-minimal supersymmetric extension of the standard model (NMSSM) [6–9] the parameter μ arises as the vacuum expectation value of the neutral component of an additional Higgs field S which is a singlet field with respect to the SM gauge groups. It couples to the MSSM Higgs fields via the interaction term $\lambda S\ (H_u \epsilon H_d)$. With the scalar field S acquiring a nonzero vacuum expectation value (VEV) $v_s/\sqrt{2}$ an effective μ term is generated with a value of the order of the SUSY-breaking scale, $\mu = \lambda\langle S\rangle \equiv \lambda v_s/\sqrt{2}$. Furthermore, new contributions to the quartic coupling increase the tree-level mass value of the lightest Higgs boson. In the MSSM the tree-level mass of the lightest Higgs boson is predicted to be below the mass of the Z boson. Large radiative corrections involving top and stop loops are necessary to lift the Higgs mass value beyond the lower bound from direct searches at LEP [10]. The additional NMSSM contributions lift the mass of the SM-like Higgs boson more easily beyond the LEP bound.

The extension of the Higgs sector by two more degrees of freedom through the introduction of an additional singlet superfield field $\hat{S}$[1] leads to a total of 7 Higgs bosons after electroweak symmetry breaking, three neutral CP-even, two neutral CP-odd and two charged Higgs bosons. The fermionic component of $\hat{S}$ mixes with the MSSM higgsinos and neutral gauginos to yield five neutralinos. Among the considerable phenomenological modifications in the Higgs and neutralino sector compared to the MSSM are possible new Higgs-to-Higgs decays, as *e.g.* the decay of a SM-like scalar Higgs boson into a pair of lighter pseudoscalar Higgs states, so that the present Tevatron and LHC search studies for supersymmetric Higgs particles have to be revisited [11]. Such a Higgs boson could have escaped the LEP bounds [12].

From the above discussions it is clear that the precise knowledge of the Higgs boson masses is indispensable to distinguish between MSSM and NMSSM predictions, to properly define scenarios with new Higgs-to-Higgs decays within the NMSSM and to correctly interpret the experimental data. In the MSSM, where radiative corrections are

[*]On leave from: Albert-Ludwigs-Universität Freiburg, Physikalisches Institut, Freiburg, Germany.

[1]We denote superfields by a hat over the field. Fields without hat are the corresponding component fields.

crucial to accommodate the light Higgs boson mass with the LEP limits, the Higgs boson masses have been calculated with impressive accuracy. After the calculation of the dominant one-loop contributions due to top/stop loops [13] the full one-loop corrections have been provided in [14]. The leading logarithmic two-loop effects obtained through renormalization group equations [15] have been completed by the genuine $\mathcal{O}(\alpha_t\alpha_s)$ [16–20], $\mathcal{O}(\alpha_t^2)$ [16,19,21], $\mathcal{O}(\alpha_b\alpha_s)$ [22] and $\mathcal{O}(\alpha_t\alpha_b + \alpha_b^2)$ [23] two-loop corrections in the limit of zero external momentum. The electroweak two-loop effects including part of the external momentum dependence have been calculated [24] and the leading three-loop contributions have been evaluated in [25]. Also in the case of a *CP*-violating MSSM a great effort has been undertaken to calculate the higher-order corrections. After first investigations [26], they have been evaluated at one-loop order in the effective potential approach [27] and with the renormalization group improved effective potential method through next-to-leading order [28]. In the Feynman diagrammatic approach the one-loop leading m_t^4 corrections have been provided in [29], a full one-loop calculation in [30], and more recently the leading two-loop contributions of $\mathcal{O}(\alpha_t\alpha_s)$ have been evaluated in [31]. The corrections have been implemented in the public computer code `FeynHiggs` [18,30,32]. `CPsuperH` [33], another public code, is based on the renormalization group improved effective potential approach [28]. The MSSM Higgs mass spectrum for real parameters can also be obtained from the spectrum calculators [34–37].

In the NMSSM, however, the higher-order calculations to the Higgs boson masses have not yet reached the same level of accuracy as in the MSSM. The leading one-loop contributions due to top/stop and bottom/sbottom loops have been calculated in the effective potential approach [38], the one-loop contributions due to chargino, neutralino and scalar loops have been evaluated in leading logarithmic order in Ref. [39]. These corrections and the leading logarithmic two-loop terms of $\mathcal{O}(\alpha_t\alpha_s)$ and $\mathcal{O}(\alpha_t^2)$, taken over from the MSSM results, have been implemented in the public computer code `NMHDECAY` [40]. Furthermore, the full one-loop contributions have been computed in the $\overline{\text{DR}}$ renormalization scheme [37,41] and the $\mathcal{O}(\alpha_t\alpha_s + \alpha_b\alpha_s)$ corrections have been provided in the approximation of zero external momentum [41]. They have been implemented in `NMHDECAY` as well as in the spectrum calculator `SPheno` [36,37].

In this paper we complement the effort to reach a higher level of accuracy in the computation of the NMSSM Higgs boson masses by providing the full one-loop corrections in a mixed $\overline{\text{DR}}$—on-shell and in an on-shell (OS) renormalization scheme. By comparison with the results of Ref. [41] in the $\overline{\text{DR}}$ scheme, the dependence on the renormalization schemes can be studied. In this way an estimate of the theoretical error due to missing higher-order corrections can be derived. Having available the corrections in the mixed and in the OS renormalization scheme in addition enables a comparison of the NMSSM results in the MSSM limit with the corresponding MSSM corrections given in the OS-scheme.

The paper is organized as follows. In Sec. II we present the details of our calculation starting by introducing the NMSSM Higgs sector and setting up our notation in II A. After presenting the chargino and neutralino sector in II B we list the parameters that we employ in Sec. II C. The renormalization is explained in detail in Sec. II D. The explicit computation of the one-loop corrected Higgs boson masses and mixing matrix elements is described in Sec. II E. Section III finally is devoted to the numerical analysis. Our results are summarized in Sec. IV.

II. CALCULATION

A. The NMSSM Higgs boson sector

The Higgs mass matrix is obtained from the NMSSM Higgs potential, which is derived from the NMSSM superpotential W_{NMSSM}, the corresponding soft SUSY breaking terms and the D term contributions. The NMSSM superpotential for the Higgs superfields $\hat{H}_u$, $\hat{H}_d$, $\hat{S}$ in our conventions reads

$$W_{\text{NMSSM}} = W_{\text{MSSM}} - \epsilon_{ab}\lambda\hat{S}\hat{H}_d^a\hat{H}_u^b + \frac{1}{3}\kappa\hat{S}^3, \qquad (1)$$

where $a, b = 1, 2$ are the $SU(2)_L$ fundamental representation indices and ϵ_{ab} denotes the totally antisymmetric tensor with $\epsilon_{12} = \epsilon^{12} = 1$. The Higgs superfield which couples to up-type (down-type) fermion superfields is given by $\hat{H}_{u(d)}$. The parameters λ and κ are dimensionless and, working in the *CP*-invariant NMSSM, are chosen to be real. The first term in Eq. (1) is the MSSM superpotential, which in terms of the quark and lepton superfields $\hat{Q}$, $\hat{U}^c$, $\hat{D}^c$, $\hat{L}$, $\hat{E}^c$ reads[2]

$$W_{\text{MSSM}} = \epsilon_{ab}[y_e\hat{H}_d^a\hat{L}^b\hat{E}^c + y_d\hat{H}_d^a\hat{Q}^b\hat{D}^c - y_u\hat{H}_u^a\hat{Q}^b\hat{U}^c], \qquad (2)$$

where we have omitted color and generation indices. Note that the MSSM μ term in NMSSM constructions is commonly assumed to be zero as well as terms linear and quadratic in $\hat{S}$. The soft SUSY breaking terms in the NMSSM in terms of the component fields H_u, H_d, S are given by

$$\mathcal{L}_{\text{soft}} = \mathcal{L}_{\text{soft,MSSM}} - m_S^2|S|^2 + \left(\epsilon_{ab}\lambda A_\lambda S H_d^a H_u^b - \frac{1}{3}\kappa A_\kappa S^3 + \text{H.c.}\right), \qquad (3)$$

with the MSSM soft SUSY breaking Lagrangian

[2]The superscript c denotes charge conjugation.

$$\begin{aligned}\mathcal{L}_{\text{soft,MSSM}} = & -m_{H_d}^2 H_d^\dagger H_d - m_{H_u}^2 H_u^\dagger H_u - m_{\tilde{Q}}^2 \tilde{Q}^\dagger \tilde{Q} \\ & - m_{\tilde{L}}^2 \tilde{L}^\dagger \tilde{L} - m_{\tilde{U}}^2 \tilde{u}_R^* \tilde{u}_R - m_{\tilde{D}}^2 \tilde{d}_R^* \tilde{d}_R - m_{\tilde{E}}^2 \tilde{e}_R^* \tilde{e}_R \\ & - (\epsilon_{ab}[y_e A_e H_d^a \tilde{L}^b \tilde{e}_R^* + y_d A_d H_d^a \tilde{Q}^b \tilde{d}_R^* \\ & - y_u A_u H_u^a \tilde{Q}^b \tilde{u}_R^*] + \text{H.c.}) \\ & - \frac{1}{2}(M_1 \tilde{B}\tilde{B} + M_2 \tilde{W}_i \tilde{W}_i + M_3 \tilde{G}\tilde{G} + \text{H.c.}), \end{aligned} \quad (4)$$

where in the first four lines tilde denotes the scalar component of the corresponding quark and lepton superfield, and $\tilde{Q} = (\tilde{u}_L, \tilde{d}_L)^T$, $\tilde{L} = (\tilde{\nu}_L, \tilde{e}_L)^T$. Note that *e.g.* $\tilde{u}_R^*$ is the scalar component of $\hat{U}^c$. In the last line the soft SUSY breaking gaugino mass terms for the gaugino fields $\tilde{B}$, $\tilde{W}_i$ ($i = 1, 2, 3$) and $\tilde{G}$ are given. All soft SUSY breaking trilinear couplings A_k ($k = \lambda, \kappa, d, u, e$) and gaugino mass parameters M_i ($i = 1, 2, 3$) are assumed to be real, and squark and slepton mixing between the generations is neglected. Furthermore, possible soft SUSY breaking terms linear and quadratic in the singlet field S are set to zero in accordance with the majority of phenomenological NMSSM constructions.[3]

The neutral components of the Higgs fields can be parametrized in terms of CP-even and CP-odd fluctuations around their vacuum expectation values,

$$\begin{aligned} H_d^1 = \frac{1}{\sqrt{2}}(v_d + h_d + i a_d), \quad H_u^2 = \frac{1}{\sqrt{2}}(v_u + h_u + i a_u), \\ S = \frac{1}{\sqrt{2}}(v_s + h_s + i a_s), \end{aligned} \quad (5)$$

with the VEVs v_d, v_u, v_s chosen to be real and positive. The parameter μ then arises dynamically from the singlet field expanded about its VEV, *cf.* Eq. (1),

$$\mu = \frac{\lambda v_s}{\sqrt{2}}. \quad (6)$$

The minimization conditions of the tree-level scalar potential can be applied to replace the soft SUSY breaking Higgs mass parameters $m_{H_u}^2$, $m_{H_d}^2$, m_S^2 by combinations of λ, κ, the electroweak gauge couplings g and g', the VEVs and the trilinear couplings A_λ, A_κ, so that the tree-level mass matrix M_S^2 of the neutral CP-even Higgs bosons obtained from the second derivative of the Higgs potential with respect to the fields in the vacuum, in the basis $h^S = (h_d, h_u, h_s)^T$ can be cast into the form

$$M_S^2 = \begin{pmatrix} \bar{g}^2 v_d^2 + \frac{(R_\lambda + R v_s/2) v_u v_s}{v_d} & (\lambda^2 - \bar{g}^2) v_u v_d - (R_\lambda + R v_s/2) v_s & \lambda^2 v_d v_s - (R_\lambda + R v_s) v_u \\ (\lambda^2 - \bar{g}^2) v_u v_d - (R_\lambda + R v_s/2) v_s & \bar{g}^2 v_u^2 + \frac{(R_\lambda + R v_s/2) v_d v_s}{v_u} & \lambda^2 v_u v_s - (R_\lambda + R v_s) v_d \\ \lambda^2 v_d v_s - (R_\lambda + R v_s) v_u & \lambda^2 v_u v_s - (R_\lambda + R v_s) v_d & 2\kappa^2 v_s^2 + \frac{R_\lambda v_u v_d}{v_s} + R_\kappa v_s \end{pmatrix} \quad (7)$$

where we have defined

$$\begin{aligned} \bar{g}^2 &= \frac{1}{4}(g^2 + g'^2), & R &= \lambda\kappa, \\ R_\lambda &= \frac{1}{\sqrt{2}}\lambda A_\lambda, & R_\kappa &= \frac{1}{\sqrt{2}}\kappa A_\kappa. \end{aligned} \quad (8)$$

Note, that the MSSM limit can be recovered by $\lambda, \kappa \to 0$ (with the ratio κ/λ kept constant for a smooth approach) and keeping the parameter $\mu = \lambda v_s/\sqrt{2}$ as well as the parameters A_λ and A_κ fixed. In this limit we hence have $v_s \to \infty$.

The CP-even mass eigenstates H_i ($i = 1, 2, 3$) are obtained by an orthogonal transformation $\mathcal{R}^S$ (the summation over paired indices is implicit),

$$H_i = \mathcal{R}_{ij}^S h_j^S. \quad (9)$$

They are ordered by ascending mass with $M_{H_1} \leq M_{H_2} \leq M_{H_3}$. The CP-odd fields (a_d, a_u, a_s) can be rotated first to separate a massless Goldstone boson G

$$\begin{pmatrix} a \\ a_s \\ G \end{pmatrix} = \begin{pmatrix} s_{\beta_n} & c_{\beta_n} & 0 \\ 0 & 0 & 1 \\ c_{\beta_n} & -s_{\beta_n} & 0 \end{pmatrix} \begin{pmatrix} a_d \\ a_u \\ a_s \end{pmatrix}, \quad (10)$$

with the abbreviations $c_x \equiv \cos x$ and $s_x \equiv \sin x$, in the following also $t_x \equiv \tan x$. Starting from the tree-level CP-odd mass matrix squared in the basis $(a_d, a_u, a_s)^T$ and using Eq. (10) results in the mass matrix squared M_P^2 in the basis $h^P = (a, a_s, G)^T$, which reads

$$M_P^2 = \begin{pmatrix} (2R_\lambda + R v_s) v_s \frac{c_{\Delta\beta}^2}{s_{2\beta}} & (R_\lambda - R v_s) v c_{\Delta\beta} & (R_\lambda + R v_s/2) v_s \frac{s_{2\Delta\beta}}{s_{2\beta}} \\ (R_\lambda - R v_s) v c_{\Delta\beta} & (2R + R_\lambda/v_s)\frac{v^2 s_{2\beta}}{2} - 3R_\kappa v_s & (R_\lambda - R v_s) v s_{\Delta\beta} \\ (R_\lambda + R v_s/2) v_s \frac{s_{2\Delta\beta}}{s_{2\beta}} & (R_\lambda - R v_s) v s_{\Delta\beta} & (2R_\lambda + R v_s) v_s \frac{s_{\Delta\beta}^2}{s_{2\beta}} \end{pmatrix} \quad (11)$$

[3]In the MSSM there is an additional soft SUSY breaking term $m_{H_d H_u}^2 \epsilon_{ab} H_d^a H_u^b$ with $m_{H_d H_u}^2$ usually expressed in terms of the soft SUSY breaking parameter B and the higgsino parameter μ as $m_{H_d H_u}^2 = B\mu$. This term is not explicitly added to the NMSSM soft SUSY breaking Lagrangian but is generated dynamically via the term $\epsilon_{ab}\lambda A_\lambda S H_d^a H_u^b$.

with $\Delta\beta = \beta - \beta_n$ and $v^2 \equiv v_u^2 + v_d^2$. The angle β_n coincides at tree-level with the angle β defined through the ratio of the VEVs v_u, v_d, $\tan\beta = v_u/v_d$. Hence $\Delta\beta = 0$ at tree-level leading to a massless Goldstone boson, which decouples as it should. The first entry $(M_P^2)_{11}$ at tree-level,

$$(M_P^2)_{11} = \frac{(2R_\lambda + Rv_s)v_s}{s_{2\beta}}, \tag{12}$$

becomes the mass of the pseudoscalar Higgs boson in the MSSM limit.[4] Applying an orthogonal rotation $\mathcal{R}^P$ to $h^P = (a, a_s, G)^T$, the CP-odd mass eigenstates $A_i \equiv A_1$, A_2, G ($i = 1, 2, 3$) are obtained,

$$A_i = \mathcal{R}_{ij}^P h_j^P, \tag{13}$$

where at tree-level $\mathcal{R}_{33}^P = 1$ and $\mathcal{R}_{3i}^P = \mathcal{R}_{i3}^P = 0$ for $i \neq 3$. The pseudoscalar masses are ordered by ascending mass, $M_{A_1} \leq M_{A_2}$. The CP-even and CP-odd Higgs mass values squared are given by the eigenvalues of the respective mass matrices M_S^2 and M_P^2. Analytic expressions would be rather complicated if not expanded in special parameter regions as *e.g.* in Ref. [42], where a comprehensive investigation of the NMSSM Higgs boson sector has been performed. In our analysis the mass eigenvalues are derived numerically. The charged Higgs boson mass on the other hand takes a simple form after the massless charged Goldstone boson has been separated by an orthogonal rotation with a mixing angle β_c. At Born level we have $\beta_c = \beta$ and get

$$\begin{aligned} M_{H^\pm}^2 &= M_W^2 + \sqrt{2}\lambda\frac{v_s}{s_{2\beta}}\left(A_\lambda + \kappa\frac{v_s}{\sqrt{2}}\right) - \frac{\lambda^2 v^2}{2} \\ &= M_W^2 + (M_P^2)_{11} - \frac{\lambda^2 v^2}{2}, \end{aligned} \tag{14}$$

with M_W being the W boson mass and where we have applied the definition given in Eq. (12).

B. The neutralino and chargino sector

The chargino sector remains unchanged with respect to the MSSM. For completeness and to set up our notation we briefly repeat the chargino system. The chargino mass matrix depends on the wino mass parameter M_2, the effective Higgsino parameter $\mu = \lambda v_s/\sqrt{2}$ and the ratio of the vacuum expectation values $\tan\beta$. In the interaction eigenbasis it is given by [43]

$$M_C = \begin{pmatrix} M_2 & \sqrt{2}M_W s_\beta \\ \sqrt{2}M_W c_\beta & \mu \end{pmatrix}. \tag{15}$$

It is diagonalized by two real matrices U and V,

$$U^* M_C V^\dagger \rightarrow U = \mathcal{O}_- \text{ and } V = \begin{cases} \mathcal{O}_+ & \text{if } \det M_C > 0 \\ \sigma_3 \mathcal{O}_+ & \text{if } \det M_C < 0 \end{cases}, \tag{16}$$

with the Pauli matrix σ_3 to render the chargino masses positive. The rotation matrices $\mathcal{O}_\pm$ are given in terms of the mixing angles

$$\begin{aligned} \tan 2\theta_- &= \frac{2\sqrt{2}M_W(M_2 c_\beta + \mu s_\beta)}{M_2^2 - \mu^2 - 2M_W^2 c_\beta}, \\ \tan 2\theta_+ &= \frac{2\sqrt{2}M_W(M_2 s_\beta + \mu c_\beta)}{M_2^2 - \mu^2 + 2M_W^2 c_\beta}, \end{aligned} \tag{17}$$

and the two chargino masses read

$$\begin{aligned} m_{\chi_{1,2}^\pm}^2 = \frac{1}{2}\Big\{ & M_2^2 + \mu^2 + 2M_W^2 \mp [(M_2^2 - \mu^2)^2 \\ & + 4M_W^2(M_W^2 c_{2\beta}^2 + M_2^2 + \mu^2 + 2M_2\mu s_{2\beta})]^{1/2} \Big\}. \end{aligned} \tag{18}$$

In the neutralino sector, the mixing of the fermionic component of the singlet superfields $\hat{S}$ with the neutral gauginos $\tilde{B}$, $\tilde{W}_3$ and higgsinos $\tilde{H}_d^0$, $\tilde{H}_u^0$ yields in the Weyl spinor basis $\psi^0 = (\tilde{B}, \tilde{W}_3, \tilde{H}_d^0, \tilde{H}_u^0, \tilde{S})^T$ the 5×5 neutralino mass matrix

$$M_N = \begin{pmatrix} M_1 & 0 & -c_\beta s_W M_Z & s_\beta s_W M_Z & 0 \\ 0 & M_2 & c_\beta c_W M_Z & -s_\beta c_W M_Z & 0 \\ -c_\beta s_W M_Z & c_\beta c_W M_Z & 0 & -\lambda v_s/\sqrt{2} & -\lambda v_u/\sqrt{2} \\ s_\beta s_W M_Z & -s_\beta c_W M_Z & -\lambda v_s/\sqrt{2} & 0 & -\lambda v_d/\sqrt{2} \\ 0 & 0 & -\lambda v_u/\sqrt{2} & -\lambda v_d/\sqrt{2} & \sqrt{2}\kappa v_s \end{pmatrix}. \tag{19}$$

We have introduced the short-hand notation $s_W \equiv \sin\theta_W$, $c_W \equiv \cos\theta_W$ for the Weinberg angle θ_W, and M_Z denotes the Z boson mass. Diagonalization with a unitary matrix $\mathcal{N}$ yields the five neutralino mass eigenstates χ_i^0 ($i = 1, \ldots, 5$),

$$\chi_i^0 = \mathcal{N}_{ij}\psi_j^0, \qquad j = 1, \ldots, 5. \tag{20}$$

They are ordered by ascending mass, $m_{\chi_1^0} \leq \ldots \leq m_{\chi_5^0}$. With our assumption of CP invariance and allowing for negative neutralino mass eigenvalues, the rotation matrix $\mathcal{N}$ is real.

C. Parameter basis

The NMSSM Higgs potential depends on 12 independent parameters in the CP-conserving case. They are given by the soft SUSY breaking mass parameters $m_{H_u}^2$, $m_{H_d}^2$, m_S^2,

[4] A_λ takes the role of the soft SUSY breaking parameter B in the MSSM.

the gauge couplings g, g', the vacuum expectation values v_u, v_d, v_s, the dimensionless parameters λ, κ and the soft SUSY breaking couplings A_λ, A_κ. For the physical interpretation it is convenient to replace some of these parameters: The minimization of the Higgs potential V requires the terms linear in the Higgs fields to vanish in the vacuum. Hence for the scalar fields,

$$\left\langle \frac{\partial V}{\partial h_u} \right\rangle = \left\langle \frac{\partial V}{\partial h_d} \right\rangle = \left\langle \frac{\partial V}{\partial h_s} \right\rangle = 0, \tag{21}$$

where the brackets denote the vacuum. The corresponding coefficients, which are called tadpoles, therefore have to be zero. At lowest order the tadpole conditions for the CP-even fields read[5]

$$\left\langle \frac{\partial V}{\partial h_d} \right\rangle \equiv t_{h_d} = v_d m_{H_d}^2 - R_\lambda v_u v_s + \frac{g^2 + g'^2}{8} v_d (v_d^2 - v_u^2) + \frac{\lambda^2}{2} v_d (v_u^2 + v_s^2) - \frac{R}{2} v_u v_s^2 = 0 \tag{22}$$

$$\left\langle \frac{\partial V}{\partial h_u} \right\rangle \equiv t_{h_u} = v_u m_{H_u}^2 - R_\lambda v_d v_s + \frac{g^2 + g'^2}{8} v_u (v_u^2 - v_d^2) + \frac{\lambda^2}{2} v_u (v_d^2 + v_s^2) - \frac{R}{2} v_d v_s^2 = 0 \tag{23}$$

$$\left\langle \frac{\partial V}{\partial h_s} \right\rangle \equiv t_{h_s} = v_s m_S^2 - R_\lambda v_d v_u + R_\kappa v_s^2 + \frac{\lambda^2}{2} v_s (v_d^2 + v_u^2) + \kappa^2 v_s^3 - R v_d v_u v_s = 0. \tag{24}$$

Equations (22)–(24), can be exploited to replace $m_{H_u}^2$, $m_{H_d}^2$, m_S^2 by the tadpole parameters t_{h_u}, t_{h_d} and t_{h_s}. The parameters g, g', v_u, v_d are replaced by the electric charge e, the gauge boson masses M_W, M_Z and the ratio of the vacuum expectation values $\tan\beta \equiv t_\beta = v_u/v_d$ through the relations

$$g = \frac{eM_Z}{\sqrt{M_Z^2 - M_W^2}} \qquad g' = \frac{eM_Z}{M_W} \tag{25}$$

$$v_u = \sqrt{\frac{M_Z^2 - M_W^2}{1 + t_\beta^2}} \frac{2M_W t_\beta}{eM_Z} \qquad v_d = \sqrt{\frac{M_Z^2 - M_W^2}{1 + t_\beta^2}} \frac{2M_W}{eM_Z}. \tag{26}$$

Finally, A_λ is replaced by the charged Higgs boson mass $M_{H^\pm}^2$,

$$A_\lambda = \frac{s_{2\beta}}{\sqrt{2}\lambda v_s} \left(\frac{v^2 \lambda^2}{2} - M_W^2 + \frac{M_{\mathrm{H}^\pm}^2}{c_{\Delta\beta}^2} \right) - \frac{\kappa v_s}{\sqrt{2}} - \frac{\sqrt{2}}{\lambda v v_s} \left(\frac{s_\beta s_{\beta_B}^2}{c_{\Delta\beta}^2} t_{h_d} + \frac{c_\beta c_{\beta_B}^2}{c_{\Delta\beta}^2} t_{h_u} \right) \tag{27}$$

with

$$v = \frac{2M_W}{e} \sqrt{1 - \frac{M_W^2}{M_Z^2}}, \tag{28}$$

where we have kept the dependence on the tadpole parameters and the mixing angles $\beta_c = \beta_n \equiv \beta_B$. At tree-level they coincide with β. It is the angle β which will be needed for the renormalization: According to our renormalization schemes, presented in Sec. II D, the renormalization procedure can be performed before the transformation into mass eigenstates. This means that the mixing matrices, also those separating the neutral and charged Goldstone bosons from the Higgs bosons and hence the angles β_n and β_c, which appear in these matrices, do not receive counterterms. Therefore, special care has to be taken to determine the elements of the mass matrices without inserting the tree-level relation $\beta_B = \beta$ and to apply the renormalization procedure uniquely for $\tan\beta$ given by the ratio of v_u and v_d.

To summarize, we work with the following parameter set

$$t_{h_u}, t_{h_d}, t_{h_s}, e, M_W^2, M_Z^2, \tan\beta, M_{H^\pm}^2, \lambda, \kappa, v_s, A_\kappa. \tag{29}$$

D. Renormalization schemes

For the determination of the loop-corrected Higgs boson masses the Higgs self-energies have to be calculated. They develop ultraviolet (UV) divergences. Evaluating the self-energies in $D = 4 - 2\epsilon$ dimensions, the divergences can be parametrized by $1/\epsilon$ leading to poles in $D = 4$ dimensions. To get a finite result the parameters entering the loop calculation have to be renormalized by the introduction of appropriate counterterms absorbing the UV divergences. Note, that at higher orders also the terms linear in the Higgs fields get loop contributions. Therefore, also the tadpole parameters t_{h_i} ($i = u, d, s$) have to be renormalized, in order to fulfill the tadpole conditions Eq. (21). Before we describe the determination of the one-loop corrected Higgs boson masses in Sec. II E, the renormalization schemes which have been adopted, shall be presented in detail in the following.

We start with a renormalization scheme which is a mixture between on-shell and $\overline{\mathrm{DR}}$ renormalization conditions. In order to make contact and to compare to earlier results presented in Ref. [41] our result will also be converted to a pure $\overline{\mathrm{DR}}$ scheme. To get an estimate of the

[5] As we work in the real NMSSM the derivatives of the Higgs potential with respect to the CP-odd fields are zero and no additional conditions have to be required.

uncertainties due to missing higher-order corrections we study the influence of the renormalization scheme on the one-loop Higgs mass corrections. We therefore also compare to a pure OS-scheme. In all three renormalization schemes, mixed, $\overline{\text{DR}}$ and OS, we start out from the parameter set Eq. (29) and replace the parameters by the renormalized ones and their corresponding counterterms,

$$\begin{aligned} &M_Z^2 \to M_Z^2 + \delta M_Z^2, \quad M_W^2 \to M_W^2 + \delta M_W^2, \\ &\quad M_{H^\pm}^2 \to M_{H^\pm}^2 + \delta M_{H^\pm}^2, \\ &t_{h_u} \to t_{h_u} + \delta t_{h_u}, \quad t_{h_d} \to t_{h_d} + \delta t_{h_d}, \quad t_{h_s} \to t_{h_s} + \delta t_{h_s}, \\ &e \to (1 + \delta Z_e) e, \quad \tan\beta \to \tan\beta + \delta\tan\beta, \quad \lambda \to \lambda + \delta\lambda, \\ &\kappa \to \kappa + \delta\kappa, \quad v_s \to v_s + \delta v_s, \quad A_\kappa \to A_\kappa + \delta A_\kappa. \end{aligned} \tag{30}$$

For the field renormalization, the Higgs boson doublet and singlet fields are replaced by the renormalized ones and a corresponding single field renormalization constant for each doublet and the singlet, respectively,

$$\begin{aligned} H_u \to \sqrt{Z_{H_u}} H_u &= \left(1 + \frac{1}{2}\delta Z_{H_u}\right) H_u \\ H_d \to \sqrt{Z_{H_d}} H_d &= \left(1 + \frac{1}{2}\delta Z_{H_d}\right) H_d \\ S \to \sqrt{Z_S} S &= \left(1 + \frac{1}{2}\delta Z_S\right) S. \end{aligned} \tag{31}$$

Applying this renormalization procedure, the renormalized self-energies in the basis $\{h_i^S | i = 1, 2, 3\} = \{h_d, h_u, h_s\}$ for the *CP*-even Higgs bosons and in the basis $\{h_i^P | i = 1, 2, 3\} = \{a, a_s, G\}$ for the *CP*-odd ones can be derived as ($X = S, P$)

$$\begin{aligned} \hat{\Sigma}_{h_i^X h_j^X}(k^2) = \Sigma_{h_i^X h_j^X}(k^2) &+ \frac{1}{2} k^2 [\delta Z_{h_j^X h_i^X} + \delta Z_{h_i^X h_j^X}] \\ &- \frac{1}{2} [\delta Z_{h_k^X h_i^X} (M_X^2)_{kj} + (M_X^2)_{ik} \delta Z_{h_k^X h_j^X}] - \delta (M_X^2)_{ij} \\ &\text{with} \quad i, j = 1, 2, 3, \end{aligned} \tag{32}$$

where

$$\begin{aligned} &\delta Z_{h_1^S h_1^S} = \delta Z_{H_d}, \quad \delta Z_{h_2^S h_2^S} = \delta Z_{H_u}, \\ &\delta Z_{h_3^S h_3^S} = \delta Z_S, \quad \delta Z_{h_i^S h_j^S} = 0 \ \text{ for } i \neq j, \end{aligned} \tag{33}$$

and

$$\begin{aligned} \delta Z_{h_1^P h_1^P} = s_\beta^2 \delta Z_{H_d} + c_\beta^2 \delta Z_{H_u}, \quad \delta Z_{h_2^P h_2^P} = \delta Z_S, \\ \delta Z_{h_3^P h_3^P} = c_\beta^2 \delta Z_{H_d} + s_\beta^2 \delta Z_{H_u} \end{aligned} \tag{34}$$

$$\delta Z_{h_1^P h_3^P} = \delta Z_{h_3^P h_1^P} = s_\beta c_\beta (\delta Z_{H_d} - \delta Z_{H_u}), \tag{35}$$

$$\delta Z_{h_1^P h_2^P} = \delta Z_{h_2^P h_1^P} = \delta Z_{h_2^P h_3^P} = \delta Z_{h_3^P h_2^P} = 0. \tag{36}$$

Here, M_S^2 and M_P^2 are the tree-level *CP*-even and *CP*-odd Higgs boson mass matrices squared, respectively. For the derivation of the counterterm matrices $\delta(M_S^2)$ and $\delta(M_P^2)$, the *CP*-even and *CP*-odd Higgs boson mass matrices squared are expressed in terms of the parameter set Eq. (29) including also their dependence on the tadpole parameters as well as on the mixing angle β_B. As the expressions are quite lengthy they are given in Appendix A. Then, the parameters entering these matrices are replaced according to Eqs. (30) and an expansion about the counterterms is performed. The part of M_S^2 and M_P^2, respectively, which is linear in the counterterms, corresponds to $\delta(M_S^2)$ and $\delta(M_P^2)$.

The renormalized self energies in Eq. (32) are related to the ones in the basis of the mass eigenstates through, *cf.* Eqs. (9) and (13),

$$\hat{\Sigma}_{H_i H_j}(k^2) = \mathcal{R}_{ik}^S \mathcal{R}_{jl}^S \hat{\Sigma}_{h_k^S h_l^S}(k^2) \tag{37}$$

$$\hat{\Sigma}_{A_i A_j}(k^2) = \mathcal{R}_{ik}^P \mathcal{R}_{jl}^P \hat{\Sigma}_{h_k^P h_l^P}(k^2) \ \text{ with } \ i, j, k, l = 1, 2, 3. \tag{38}$$

The field renormalization constants δZ_{H_d}, δZ_{H_u}, δZ_S are obtained from

$$\begin{aligned} \delta Z_{H_i H_i} = |\mathcal{R}_{i1}^S|^2 \delta Z_{H_d} + |\mathcal{R}_{i2}^S|^2 \delta Z_{H_u} \\ + |\mathcal{R}_{i3}^S|^2 \delta Z_S, \qquad i = 1, 2, 3, \end{aligned} \tag{39}$$

with

$$\delta Z_{H_i H_i} = -\frac{\partial \Sigma_{H_i H_i}(k^2)}{\partial k^2}\bigg|^{\text{div}}_{k^2 = (M_{H_i}^{(0)})^2}, \qquad i = 1, 2, 3, \tag{40}$$

where $(M_{H_i}^{(0)})^2$ denotes the corresponding tree-level mass squared. The field renormalization constants are defined in all three renormalization schemes via $\overline{\text{DR}}$ conditions. This is indicated by the superscript 'div' and means that in the field renormalization only the divergent part $\Delta = 2/(4 - D) - \gamma_E + \ln(4\pi)$ is kept with γ_E being the Euler constant. Solving Eq. (39) for δZ_{H_d}, δZ_{H_u}, δZ_S results in

$$\begin{aligned} \delta Z_{H_d} = [&(|\mathcal{R}_{23}^S|^2 |\mathcal{R}_{32}^S|^2 - |\mathcal{R}_{22}^S|^2 |\mathcal{R}_{33}^S|^2) \delta Z_{H_1 H_1} \\ &+ (|\mathcal{R}_{12}^S|^2 |\mathcal{R}_{33}^S|^2 - |\mathcal{R}_{13}^S|^2 |\mathcal{R}_{32}^S|^2) \delta Z_{H_2 H_2} \\ &+ (|\mathcal{R}_{13}^S|^2 |\mathcal{R}_{22}^S|^2 - |\mathcal{R}_{12}^S|^2 |\mathcal{R}_{23}^S|^2) \delta Z_{H_3 H_3}]/R_r^S \end{aligned} \tag{41}$$

$$\begin{aligned} \delta Z_{H_u} = [&(|\mathcal{R}_{21}^S|^2 |\mathcal{R}_{33}^S|^2 - |\mathcal{R}_{23}^S|^2 |\mathcal{R}_{31}^S|^2) \delta Z_{H_1 H_1} \\ &+ (|\mathcal{R}_{13}^S|^2 |\mathcal{R}_{31}^S|^2 - |\mathcal{R}_{11}^S|^2 |\mathcal{R}_{33}^S|^2) \delta Z_{H_2 H_2} \\ &+ (|\mathcal{R}_{11}^S|^2 |\mathcal{R}_{23}^S|^2 - |\mathcal{R}_{13}^S|^2 |\mathcal{R}_{21}^S|^2) \delta Z_{H_3 H_3}]/R_r^S \end{aligned} \tag{42}$$

$$\begin{aligned} \delta Z_S = [&(|\mathcal{R}_{22}^S|^2 |\mathcal{R}_{31}^S|^2 - |\mathcal{R}_{21}^S|^2 |\mathcal{R}_{32}^S|^2) \delta Z_{H_1 H_1} \\ &+ (|\mathcal{R}_{11}^S|^2 |\mathcal{R}_{32}^S|^2 - |\mathcal{R}_{12}^S|^2 |\mathcal{R}_{31}^S|^2) \delta Z_{H_2 H_2} \\ &+ (|\mathcal{R}_{12}^S|^2 |\mathcal{R}_{21}^S|^2 - |\mathcal{R}_{11}^S|^2 |\mathcal{R}_{22}^S|^2) \delta Z_{H_3 H_3}]/R_r^S \end{aligned} \tag{43}$$

where

$$R_r^S = -|\mathcal{R}^S_{11}|^2|\mathcal{R}^S_{22}|^2|\mathcal{R}^S_{33}|^2 + |\mathcal{R}^S_{11}|^2|\mathcal{R}^S_{23}|^2|\mathcal{R}^S_{32}|^2 + |\mathcal{R}^S_{12}|^2|\mathcal{R}^S_{21}|^2|\mathcal{R}^S_{33}|^2 - |\mathcal{R}^S_{12}|^2|\mathcal{R}^S_{23}|^2|\mathcal{R}^S_{31}|^2 - |\mathcal{R}^S_{13}|^2|\mathcal{R}^S_{21}|^2|\mathcal{R}^S_{32}|^2 + |\mathcal{R}^S_{13}|^2|\mathcal{R}^S_{22}|^2|\mathcal{R}^S_{31}|^2. \quad (44)$$

Contrary to the field renormalization constants the renormalization conditions for the remaining parameters are different in the three chosen renormalization schemes, as will be described in the following.

Mixed renormalization scheme

In the mixed renormalization scheme we divide the parameters into parameters defined through on-shell conditions[6] and into parameters defined via $\overline{\text{DR}}$ conditions:

$$\underbrace{M_Z, M_W, M_{H^\pm}, t_{h_u}, t_{h_d}, t_{h_s}, e}_{\text{on-shell scheme}}, \underbrace{\tan\beta, \lambda, v_s, \kappa, A_\kappa}_{\overline{\text{DR}}\text{ scheme}}. \quad (45)$$

In the following, the various counterterms shall be specified in more detail.

(i,ii) Gauge boson masses

The gauge boson masses are defined through on-shell conditions,

$$\text{Re}\,\hat{\Sigma}^T_{ZZ}(M_Z^2) = 0, \qquad \text{Re}\hat{\Sigma}^T_{WW}(M_W^2) = 0, \quad (46)$$

where T denotes the transverse part of the respective self-energy. For the mass counterterms this yields

$$\delta M_Z^2 = \text{Re}\Sigma^T_{ZZ}(M_Z^2), \qquad \delta M_W^2 = \text{Re}\Sigma^T_{WW}(M_W^2). \quad (47)$$

Note, that the NMSSM gauge boson self-energies differ from the MSSM case due to the introduction of an additional superfield $\hat{S}$.

(iii) Mass of the charged Higgs boson

The mass of the charged Higgs boson is determined through the on-shell condition,

$$\text{Re}\,\hat{\Sigma}_{H^\pm H^\mp}(M^2_{H^\pm}) = 0, \quad (48)$$

resulting in the corresponding counterterm

$$\delta M^2_{H^\pm} = \text{Re}\Sigma_{H^\pm H^\mp}(M^2_{H^\pm}). \quad (49)$$

(iv-vi) Tadpole parameters

The tadpole coefficients are required to vanish also at one-loop order, yielding

$$t^{(1)}_{h_i} - \delta t_{h_i} = 0, \qquad i = d, u, s, \quad (50)$$

where $t^{(1)}_{h_i}$ stands for the contributions coming from the corresponding genuine Higgs boson tadpole graphs. As the tadpole graphs are calculated in the mass eigenstate basis, they have to be transformed to the interaction basis. Applying Eq. (9) we have

$$\delta t_{h_i} = \mathcal{R}^S_{ji} t^{(1)}_{H_j}, \qquad i = d, u, s, \qquad j = 1, 2, 3. \quad (51)$$

(vii) Electric charge

The electric charge is defined to be the full electron-positron photon coupling for on-shell external particles in the Thomson limit, so that all corrections to this vertex vanish on-shell and for zero momentum transfer. The counterterm for the electric charge is then given in terms of the transverse part of the photon-photon and photon-Z self-energies [44],[7]

$$\delta Z_e = \frac{1}{2}\frac{\partial \Sigma^T_{\gamma\gamma}(k^2)}{\partial k^2}\bigg|_{k^2=0} + \frac{s_W}{c_W}\frac{\Sigma^T_{\gamma Z}(0)}{M_Z^2}. \quad (52)$$

(viii) $\tan\beta$

For the renormalization of $\tan\beta$ we adopt the $\overline{\text{DR}}$ scheme. Applying Eq. (31) and

$$v_i \to v_i + \delta v_i \qquad i = u, d \quad (53)$$

results in

$$\delta\tan\beta = \tan\beta\left[\frac{1}{2}(\delta Z_{H_u} - \delta Z_{H_d}) + \left(\frac{\delta v_u}{v_u} - \frac{\delta v_d}{v_d}\right)\right]_{\text{div}} = \left[\frac{\tan\beta}{2}(\delta Z_{H_u} - \delta Z_{H_d})\right]_{\text{div}}, \quad (54)$$

where we have used in the last step $\delta v_u/v_u|_{\text{div}} = \delta v_d/v_d|_{\text{div}}$ [45]. The field renormalization constants δZ_{H_d} and δZ_{H_u} are given in Eqs. (41) and (42).

(ix) Coupling λ

In the mixed renormalization scheme λ is defined as a $\overline{\text{DR}}$ parameter. The counterterm is determined via the renormalized self-energy $\hat{\Sigma}_{h_1^P h_1^P}$, see Eq. (32), using that

$$\hat{\Sigma}_{h_1^P h_1^P}((M_P^2)_{11})|_{\text{div}} = 0 \iff \delta(M_P^2)_{11,\text{div}} = \Sigma_{h_1^P h_1^P}((M_P^2)_{11})|_{\text{div}}. \quad (55)$$

As $\delta(M_P^2)_{11}$ contains the counterterm $\delta\lambda$,[8] Eq. (55) can be solved for $\delta\lambda$ resulting in,

$$\delta\lambda = \frac{e^2}{4\lambda M_W^2 s_W^2}\left[\Sigma_{h_1^P h_1^P}((M_P^2)_{11}) - \delta M^2_{H^\pm} + \delta M_W^2\left(1 + \frac{2\lambda^2(c_W^2 - s_W^2)}{e^2}\right) - \frac{2\lambda^2 c_W^4}{e^2}\delta M_Z^2 + \frac{4\lambda^2 M_W^2 s_W^2}{e^2}\delta Z_e\right]_{\text{div}}. \quad (56)$$

The self-energy $\Sigma_{h_1^P h_1^P}$ is obtained from the self-energies in the mass eigenstate basis $\Sigma_{A_i A_j}$ $(i, j = 1, 2, 3)$ through

$$\Sigma_{h_1^P h_1^P} = \mathcal{R}^P_{i1}\Sigma_{A_i A_j}\mathcal{R}^P_{j1}. \quad (57)$$

[6] In slight abuse of the language we also call the renormalization conditions for the tadpole parameters on-shell.

[7] Note that the sign of the second term in Eq. (52) differs from the one in [44] due to our conventions in the Feynman rules.

[8] Compare with Eq. (12).

(x) Singlet vacuum expectation value v_s

The vacuum expectation value v_s of the singlet field is renormalized in the $\overline{\text{DR}}$ scheme. The counterterm is derived by exploiting the chargino sector. In fact, the lower right entry of the chargino mass matrix M_C in the interaction basis reads, *cf.* Eq. (15),

$$(M_C)_{22} = \frac{\lambda v_s}{\sqrt{2}}. \tag{58}$$

Applying Eq. (30), expanding around the counterterms and extracting the terms linear in the counterterms yields

$$\delta v_s = \left[\frac{\sqrt{2}}{\lambda}\delta(M_C)_{22} - v_s\frac{\delta\lambda}{\lambda}\right]_{\text{div}}, \tag{59}$$

with $\delta\lambda$ given by Eq. (56). The counterterm $\delta(M_C)_{22}$ is obtained from the renormalized chargino self-energies in the following way. Defining the general structure of a fermionic self-energy[9] as,

$$\Sigma_{ij}(k^2) = \not{k}\Sigma^L_{ij}(k^2)\mathcal{P}_L + \not{k}\Sigma^R_{ij}(k^2)\mathcal{P}_R + \Sigma^{Ls}_{ij}(k^2)\mathcal{P}_L + \Sigma^{Rs}_{ij}(k^2)\mathcal{P}_R, \tag{60}$$

where $\mathcal{P}_{L,R} = (\mathbb{1} \mp \gamma_5)/2$ are the left- and right-handed projectors, we use the condition

$$[(M_C)_{22}[V^\dagger\hat{\Sigma}^L_{\chi^\pm}(k^2)V + U^T\hat{\Sigma}^R_{\chi^\pm}(k^2)U^*]_{22} + [U^T\hat{\Sigma}^{Ls}_{\chi^\pm}(k^2)V + V^\dagger\hat{\Sigma}^{Rs}_{\chi^\pm}(k^2)U^*]_{22}]_{\text{div}} = 0. \tag{61}$$

Note that $\hat{\Sigma}_{\chi^\pm}$ is a 2×2 matrix with the entries given by the renormalized self-energies of the charginos in the mass eigenbasis. The renormalized self-energies in terms of the unrenormalized ones, the mass counterterms and field renormalization constants are given in Appendix B, Eqs. (B5)–(B8). The structure of the condition Eq. (61) has been chosen such that the (divergent) contributions of the chargino field renormalization constants drop out. Replacing the renormalized self-energy by the relations (B5)–(B8) leads to the counterterm $\delta(M_C)_{22,\text{div}}$,

$$\delta(M_C)_{22,\text{div}} = \frac{1}{2}[(M_C)_{22}[V^\dagger\Sigma^L_{\chi^\pm}(k^2)V + U^T\Sigma^R_{\chi^\pm}(k^2)U^*]_{22} + [U^T\Sigma^{Ls}_{\chi^\pm}(k^2)V + V^\dagger\Sigma^{Rs}_{\chi^\pm}(k^2)U^*]_{22}]_{\text{div}}. \tag{62}$$

Note that the k^2 dependence in Eq. (62) drops out as only the divergent part is taken.

(xi) Coupling κ

The counterterm for the $\overline{\text{DR}}$ renormalized parameter κ is derived from the neutralino sector in an analogous procedure as the chargino sector was exploited to determine δv_s. The lower right entry $(M_N)_{55}$ of the neutralino mass matrix Eq. (19) reads

$$(M_N)_{55} = \sqrt{2}\kappa v_s, \tag{63}$$

leading to the counterterm $\delta\kappa$,

$$\delta\kappa = \frac{1}{\sqrt{2}v_s}\delta(M_N)_{55} - \kappa\frac{\delta v_s}{v_s}. \tag{64}$$

The determination of δv_s has been described in the previous paragraph. For the determination of $\delta(M_N)_{55}$ we use the condition

$$[(M_N)_{55}[\mathcal{N}^T(\hat{\Sigma}^L_{\chi^0}(k^2) + \hat{\Sigma}^R_{\chi^0}(k^2))\mathcal{N}]_{55} + [\mathcal{N}^T(\hat{\Sigma}^{Ls}_{\chi^0}(k^2) + \hat{\Sigma}^{Rs}_{\chi^0}(k^2))\mathcal{N}]_{55}]_{\text{div}} = 0, \tag{65}$$

where the fermionic self-energy structure Eq. (60) has been applied for the decomposition of the renormalized neutralino 5×5 self-energy matrix $\hat{\Sigma}_{\chi^0}$. Once again the condition has been chosen such that the divergent parts of the field renormalization constants cancel in Eq. (65). Rewriting the equation in terms of the unrenormalized self-energies, *cf.* Eqs. (B9)–(B12), yields

$$\delta(M_N)_{55,\text{div}} = \frac{1}{2}[(M_N)_{55}[\mathcal{N}^T(\Sigma^L_{\chi^0}(k^2) + \Sigma^R_{\chi^0}(k^2))\mathcal{N}]_{55} + [\mathcal{N}^T(\Sigma^{Ls}_{\chi^0}(k^2) + \Sigma^{Rs}_{\chi^0}(k^2))\mathcal{N}]_{55}]_{\text{div}}, \tag{66}$$

which is inserted in Eq. (64) to determine $\delta\kappa$.

(xii) Trilinear coupling A_κ

The trilinear coupling A_κ is also defined as a $\overline{\text{DR}}$ parameter. For the derivation of the counterterm we use that

$$\hat{\Sigma}_{h_2^P h_2^P}((M_P^2)_{22})|_{\text{div}} = 0. \tag{67}$$

Equation (67) depends on δA_κ via the mass matrix squared counterterm $\delta(M_P^2)_{22}$. Solving for δA_κ we have

$$\delta A_\kappa = \left[-\frac{\sqrt{2}}{3\kappa v_s}[\Sigma_{h_2^P h_2^P}((M_P^2)_{22}) - \delta f] - A_\kappa\left[\frac{\delta\kappa}{\kappa} + \frac{\delta v_s}{v_s}\right]\right]_{\text{div}}. \tag{68}$$

The counterterm δf is derived from

$$f = \frac{t_{h_s}}{v_s} - \frac{2M_W s_W s_\beta c_\beta^2 c_{\beta_B}^2}{e v_s^2 c_{\Delta\beta}^2}[t_{h_u} + t_{h_d} t_\beta t_{\beta_B}^2] + \frac{M_W^2 s_W^2 s_{2\beta}^2}{e^2 v_s^2 c_{\Delta\beta}^2}[M_{H^\pm}^2 - M_W^2 c_{\Delta\beta}^2] + \frac{\lambda M_W^2 s_W^2 s_{2\beta}}{e^4 v_s^2}[2\lambda M_W^2 s_W^2 s_{2\beta} + 3\kappa e^2 v_s^2], \tag{69}$$

with $\Delta\beta = \beta - \beta_B$. This is done by replacing the parameters t_{h_u}, t_{h_d}, t_{h_s}, e, M_Z, M_W, $M_{H^\pm}$, $\tan\beta$, λ, κ, and v_s according to Eq. (30), performing an expansion about the counterterms, extracting the part linear in the counterterms and finally applying the tree-level relations for the tadpole parameters $t_{h_u} = t_{h_d} = t_{h_s} = 0$ and for the mixing angle, $\beta_B = \beta$.

The self-energy $\Sigma_{h_2^P h_2^P}$ in terms of the corresponding self-energies in the mass eigenbasis is given by

[9]The decomposition can be applied both for unrenormalized self-energies Σ and renormalized self-energies $\hat{\Sigma}$.

$$\Sigma_{h_2^P h_2^P} = \mathcal{R}^P_{i2}\Sigma_{A_iA_j}\mathcal{R}^P_{j2}, \qquad i,j = 1,2,3. \tag{70}$$

Alternatively, we could have derived the counterterms δv_s and $\delta\kappa$ from the Higgs sector instead of resorting to the chargino and neutralino sector. We have explicitly verified that this leads to the same results for the one-loop corrected Higgs boson masses. Our choice of renormalization allows a nontrivial cross-check of the renormalization procedure. Moreover, it paves the way for an extension of the one-loop corrections to the Higgs decays into charginos and neutralinos.

On-shell renormalization scheme

In this renormalization scheme we keep the conditions (i)–(viii) ($\tan\beta$ is still renormalized in the $\overline{\text{DR}}$ scheme) but the parameters v_s, λ, κ and A_κ are determined via on-shell renormalization conditions. This is done by applying on-shell renormalization conditions on the two CP-odd Higgs boson mass eigenstates A_1, A_2, on the mass eigenstates of the two charginos and on the mass eigenstates of the two lightest neutralinos. As OS conditions are imposed on the mass eigenstates not only single elements of the counterterm mass matrices occur in the conditions, in contrast to the $\overline{\text{DR}}$ conditions exploited within the mixed scheme. Thus, the equations get more involved and include also the parameters M_1, M_2. This is why six renormalization conditions are required, although in the end the counterterms for M_1, M_2 are not needed. Because of these OS conditions the counterterms for the parameters v_s, λ, κ and A_κ also include a finite part, which ensures that the physical masses of the particle states on which we imposed the OS conditions remain at their tree-level value even at one-loop level.

Requiring on-shell masses for the CP-odd Higgs bosons as well as for the two charginos and for the lightest and next-to-lightest neutralinos leads to the following relations,

$$\begin{aligned}
(\mathcal{R}^P\delta(M_P^2)(\mathcal{R}^P)^{\mathrm{T}})|_{11} &= \mathrm{Re}\Sigma_{A_1A_1}((M^{(0)}_{A_1})^2),\\
(\mathcal{R}^P\delta(M_P^2)(\mathcal{R}^P)^{\mathrm{T}})|_{22} &= \mathrm{Re}\Sigma_{A_2A_2}((M^{(0)}_{A_2})^2),\\
(U^*\delta(M_C)V^\dagger)|_{11} &= \frac{1}{2}\mathrm{Re}[m_{\chi_1^\pm}(\Sigma^L_{\chi_{11}^\pm}(m^2_{\chi_1^\pm}) + \Sigma^R_{\chi_{11}^\pm}(m^2_{\chi_1^\pm}))\\
&\quad + \Sigma^{Ls}_{\chi_{11}^\pm}(m^2_{\chi_1^\pm}) + \Sigma^{Rs}_{\chi_{11}^\pm}(m^2_{\chi_1^\pm})],\\
(U^*\delta(M_C)V^\dagger)|_{22} &= \frac{1}{2}\mathrm{Re}[m_{\chi_2^\pm}(\Sigma^L_{\chi_{22}^\pm}(m^2_{\chi_2^\pm}) + \Sigma^R_{\chi_{22}^\pm}(m^2_{\chi_2^\pm}))\\
&\quad + \Sigma^{Ls}_{\chi_{22}^\pm}(m^2_{\chi_2^\pm}) + \Sigma^{Rs}_{\chi_{22}^\pm}(m^2_{\chi_2^\pm})],\\
(\mathcal{N}\delta(M_N)\mathcal{N}^T)|_{11} &= \frac{1}{2}\mathrm{Re}[m_{\chi_1^0}(\Sigma^L_{\chi_{11}^0}(m^2_{\chi_1^0}) + \Sigma^R_{\chi_{11}^0}(m^2_{\chi_1^0}))\\
&\quad + \Sigma^{Ls}_{\chi_{11}^0}(m^2_{\chi_1^0}) + \Sigma^{Rs}_{\chi_{11}^0}(m^2_{\chi_1^0})],\\
(\mathcal{N}\delta(M_N)\mathcal{N}^T)|_{22} &= \frac{1}{2}\mathrm{Re}[m_{\chi_2^0}(\Sigma^L_{\chi_{22}^0}(m^2_{\chi_2^0}) + \Sigma^R_{\chi_{22}^0}(m^2_{\chi_2^0}))\\
&\quad + \Sigma^{Ls}_{\chi_{22}^0}(m^2_{\chi_2^0}) + \Sigma^{Rs}_{\chi_{22}^0}(m^2_{\chi_2^0})],
\end{aligned} \tag{71}$$

where $(M^{(0)}_{A_{1,2}})^2$ are the tree-level masses squared of the pseudoscalar mass eigenstates A_1, A_2. The counterterm matrix $\delta(M_P^2)$ is derived as described above. The entries $\delta(M_C)_{ij}$ $(i,j=1,2)$ of the counterterm matrix $\delta(M_C)$ for the charginos read

$$\delta M_{C_{11}} = \delta M_2 \tag{72}$$

$$\delta M_{C_{12}} = \delta M_W^2\frac{s_\beta}{\sqrt{2}M_W} + \delta\tan\beta\sqrt{2}c_\beta^3 M_W \tag{73}$$

$$\delta M_{C_{21}} = \delta M_W^2\frac{c_\beta}{\sqrt{2}M_W} - \delta\tan\beta\sqrt{2}c_\beta^2 M_W s_\beta \tag{74}$$

$$\delta M_{C_{22}} = \delta\lambda\frac{v_s}{\sqrt{2}} + \delta v_s\frac{\lambda}{\sqrt{2}}. \tag{75}$$

And finally, the entries $\delta(M_N)_{ij} = \delta(M_N)_{ji}$ $(i,j=1\ldots5)$ of the counterterm matrix $\delta(M_N)$ for the neutralinos can be cast into the form

$$\delta M_{N_{11}} = \delta M_1 \tag{76}$$

$$\delta M_{N_{13}} = (\delta M_W^2 - \delta M_Z^2)\frac{c_\beta}{2M_Z s_W} + \delta\tan\beta\frac{c_\beta M_Z s_W s_{2\beta}}{2} \tag{77}$$

$$\delta M_{N_{14}} = (\delta M_Z^2 - \delta M_W^2)\frac{s_\beta}{2M_Z s_W} + \delta\tan\beta\frac{c_\beta^3 M_W s_W}{c_W} \tag{78}$$

$$\delta M_{N_{22}} = \delta M_2 \tag{79}$$

$$\delta M_{N_{23}} = \delta M_W^2\frac{c_\beta}{2M_W} - \delta\tan\beta c_\beta^2 M_W s_\beta \tag{80}$$

$$\delta M_{N_{24}} = -\delta M_W^2\frac{s_\beta}{2M_W} - \delta\tan\beta c_\beta^3 M_W \tag{81}$$

$$\delta M_{N_{34}} = -\delta\lambda\frac{v_s}{\sqrt{2}} - \delta v_s\frac{\lambda}{\sqrt{2}} \tag{82}$$

$$\begin{aligned}
\delta M_{N_{35}} &= -(c_W^4\delta M_Z^2 - 2c_W^2\delta M_W^2 + \delta M_W^2)\frac{\lambda s_\beta}{\sqrt{2}eM_W s_W}\\
&\quad - \delta\tan\beta\frac{\sqrt{2}\lambda c_\beta^3 M_W s_W}{e}\\
&\quad + (\lambda\delta Z_e - \delta\lambda)\frac{\sqrt{2}M_W s_W s_\beta}{e}
\end{aligned} \tag{83}$$

$$\begin{aligned}
\delta M_{N_{45}} &= -(c_W^4\delta M_Z^2 - 2c_W^2\delta M_W^2 + \delta M_W^2)\frac{\lambda c_\beta}{\sqrt{2}eM_W s_W}\\
&\quad + \delta\tan\beta\frac{\lambda c_\beta M_W s_W s_{2\beta}}{\sqrt{2}e}\\
&\quad + (\lambda\delta Z_e - \delta\lambda)\frac{\sqrt{2}c_\beta M_W s_W}{e}
\end{aligned} \tag{84}$$

$$\delta M_{N_{55}} = \sqrt{2}\delta\kappa v_s + \sqrt{2}\kappa\delta v_s \tag{85}$$

$$\delta M_{N_{12}} = \delta M_{N_{15}} = \delta M_{N_{25}} = \delta M_{N_{33}} = \delta M_{N_{44}} = 0. \tag{86}$$

With these ingredients the explicit expressions for the Eqs. (71) can be derived. In our calculation, the system of Eqs. (71) is solved numerically, keeping, however, the dependence on the divergent part Δ explicitly.

$\overline{\text{DR}}$ *renormalization scheme*

The $\overline{\text{DR}}$ renormalization scheme differs in the conditions for the parameters $M_Z, M_W, M_{H^\pm}$ and e from the mixed one. Note that a change of the renormalization condition for $M_{H^\pm}$ can be interpreted as a change of the condition for A_λ, *cf.* Eq. (14). For these parameters instead of OS conditions $\overline{\text{DR}}$ renormalization conditions are adopted now. The other renormalization conditions do not change. So, all parameters with the exception of the tadpole parameters are renormalized using $\overline{\text{DR}}$ conditions, whereas on-shell conditions are used for the tadpole parameters.

E. Loop corrected Higgs boson masses and mixing matrix elements

The one-loop corrected scalar Higgs boson masses squared are extracted numerically as the zeroes of the determinant of the two-point vertex function $\hat{\Gamma}^S$,

$$\hat{\Gamma}^S(k^2) = i \begin{pmatrix} k^2 - (M^{(0)}_{H_1})^2 + \hat{\Sigma}_{H_1H_1}(k^2) & \hat{\Sigma}_{H_1H_2}(k^2) & \hat{\Sigma}_{H_1H_3}(k^2) \\ \hat{\Sigma}_{H_2H_1}(k^2) & k^2 - (M^{(0)}_{H_2})^2 + \hat{\Sigma}_{H_2H_2}(k^2) & \hat{\Sigma}_{H_2H_3}(k^2) \\ \hat{\Sigma}_{H_3H_1}(k^2) & \hat{\Sigma}_{H_3H_2}(k^2) & k^2 - (M^{(0)}_{H_3})^2 + \hat{\Sigma}_{H_3H_3}(k^2) \end{pmatrix}. \tag{87}$$

In the same way the pseudoscalar masses squared are obtained from $\hat{\Gamma}^P$,

$$\hat{\Gamma}^P(k^2) = i \begin{pmatrix} k^2 - (M^{(0)}_{A_1})^2 + \hat{\Sigma}_{A_1A_1}(k^2) & \hat{\Sigma}_{A_1A_2}(k^2) \\ \hat{\Sigma}_{A_2A_1}(k^2) & k^2 - (M^{(0)}_{A_2})^2 + \hat{\Sigma}_{A_2A_2}(k^2) \end{pmatrix}. \tag{88}$$

The superscript (0) denotes the tree-level values of the masses squared. It should be noted that in Eq. (88) the mixing with the Goldstone bosons is not taken into account. We have checked explicitly that the numerical effect is negligible. The unrenormalized self-energy and tadpole contributions that occur implicitly in Eqs. (87) and (88) are evaluated at one-loop order. They contain fermion, Goldstone and Higgs boson, gauge boson and ghost loops as well as loops from the corresponding superpartners *i.e.* sfermions, charginos and neutralinos.

The mass eigenvalues are obtained iteratively. In order to obtain the lightest scalar Higgs boson mass *e.g.*, in the first iteration the external momentum squared k^2 in the renormalized self-energies $\hat{\Sigma}_{H_iH_j}$ is set equal to the lightest scalar tree-level mass squared. Then, the mass matrix part of $\hat{\Gamma}^S$, meaning $(i\hat{\Gamma}^S + k^2\mathbb{1})$, is diagonalized and the resulting mass eigenvalues squared are used in the next iteration where k^2 is set equal to the lightest of the obtained mass eigenvalues. Once again the mass eigenvalues are obtained. The procedure is repeated until the deviation between the lightest eigenvalue and the one of the previous iteration is less than 10^{-9}. The other Higgs mass eigenvalues are derived accordingly.

Because of the radiative corrections, not only the masses of the particles receive contributions but also the fields are affected. To take these effects into account, new matrices, $\mathcal{R}^{S,1l}$, $\mathcal{R}^{P,1l}$, are introduced which transform the fields h_u, h_d, h_s and a, a_s into the corresponding one-loop mass eigenstates, respectively. These matrices are no physical observables and beyond lowest order they depend on the external momentum in the self-energies. For the derivation of the radiatively corrected matrices, $\mathcal{R}^{S,1l}$, $\mathcal{R}^{P,1l}$, we follow the procedure applied in Ref. [30]. It ensures the correct on-shell properties for the external particle in processes with external on-shell Higgs bosons at higher orders and thus accounts also for the mixing between the Higgs bosons. This leads to finite wave function correction factors. In the scalar case *e.g.* we have to apply the additional factor $\mathbf{Z}^S_f$ to the tree-level matrix $\mathcal{R}^S$, which rotates the interaction states $(h_d, h_u, h_s)^T$ to the mass eigenstates $(H_1, H_2, H_3)^T$, to get the one-loop matrix elements,

$$\mathcal{R}^{S,1l}_{il} = (\mathbf{Z}^S_f)_{ij}\mathcal{R}^S_{jl}, \quad i,j = H_1, H_2, H_3, \quad l = h_d, h_u, h_s. \tag{89}$$

The correction factor is given by

$$(\mathbf{Z}^S_f)_{ij} = \sqrt{\hat{Z}^S_i}\hat{Z}^S_{ij}, \tag{90}$$

with

$$\hat{Z}^S_i = \frac{1}{1 + (\text{Re}\hat{\Sigma}^{\text{eff}}_{ii})'(M_{H_i})^2}. \tag{91}$$

The prime denotes the derivative with respect to k^2, and $M^2_{H_i}$ is the one-loop corrected Higgs boson mass squared. The effective self-energy $\hat{\Sigma}^{\text{eff}}$ appears in the diagonal Higgs boson propagators

$$\Delta_{ii}(k^2) = -[(\hat{\Gamma}^S(k^2))^{-1}]_{ii} = \frac{i}{k^2 - (M^{(0)}_{H_i})^2 + \hat{\Sigma}^{\text{eff}}_{ii}(k^2)}. \tag{92}$$

It is given by (no summation over i, j, l)

$$\hat{\Sigma}^{\text{eff}}_{ii}(k^2) = \hat{\Sigma}_{ii} - i\frac{2\hat{\Gamma}^S_{ij}(k^2)\hat{\Gamma}^S_{jl}(k^2)\hat{\Gamma}^S_{li}(k^2) - (\hat{\Gamma}^S)^2_{li}(k^2)\hat{\Gamma}^S_{jj}(k^2) - (\hat{\Gamma}^S)^2_{ij}(k^2)\hat{\Gamma}^S_{ll}(k^2)}{\hat{\Gamma}^S_{jj}(k^2)\hat{\Gamma}^S_{ll}(k^2) - (\hat{\Gamma}^S)^2_{jl}(k^2)}. \tag{93}$$

The off-diagonal Higgs boson propagator Δ_{ij} ($i \neq j$, no summation over i, j, l) reads

$$\Delta_{ij}(k^2) = \frac{\hat{\Gamma}^S_{ij}\hat{\Gamma}^S_{ll} - \hat{\Gamma}^S_{jl}\hat{\Gamma}^S_{li}}{\hat{\Gamma}^S_{ii}\hat{\Gamma}^S_{jj}\hat{\Gamma}^S_{ll} + 2\hat{\Gamma}^S_{ij}\hat{\Gamma}^S_{jl}\hat{\Gamma}^S_{li} - \hat{\Gamma}^S_{ii}(\hat{\Gamma}^S)^2_{jl} - \hat{\Gamma}^S_{jj}(\hat{\Gamma}^S)^2_{ji} - \hat{\Gamma}^S_{ll}(\hat{\Gamma}^S)^2_{ij}}. \tag{94}$$

The argument k^2 in $\hat{\Gamma}^S_{ij}$ has been dropped for better readability. For $\hat{Z}^S_{ij}$ we have in terms of the propagators (again no summation over the indices)

$$\hat{Z}^S_{ij} = \frac{\Delta_{ij}(k^2)}{\Delta_{ii}(k^2)}\bigg|_{k^2=M^2_{H_i}} \overset{i\neq j}{=} \frac{\hat{\Sigma}_{ij}(M^2_{H_i})(M^2_{H_i} - (M^{(0)}_{H_l})^2 + \hat{\Sigma}_{ll}(M^2_{H_i})) - \hat{\Sigma}_{jl}(M^2_{H_i})\hat{\Sigma}_{li}(M^2_{H_i})}{\hat{\Sigma}^2_{jl}(M^2_{H_i}) - (M^2_{H_i} - (M^{(0)}_{H_j})^2 + \hat{\Sigma}_{jj}(M^2_{H_i}))(M^2_{H_i} - (M^{(0)}_{H_l})^2 + \hat{\Sigma}_{ll}(M^2_{H_i}))} \tag{95}$$

$$\hat{Z}^S_{ii} = 1. \tag{96}$$

In case of the pseudoscalar 2×2 mixing matrix $\mathcal{R}^{P,1l}_{il}$ the effective self-energy reduces to

$$\hat{\Sigma}^{\text{eff}}_{ii}(k^2) = \hat{\Sigma}_{ii} + i\frac{(\hat{\Gamma}^P)^2_{ij}(k^2)}{\hat{\Gamma}^P_{jj}(k^2)}, \qquad i,j = A_1, A_2, \tag{97}$$

and the off-diagonal propagator reads

$$\Delta_{ij}(k^2) = \frac{\hat{\Gamma}^P_{ij}}{\hat{\Gamma}^P_{ii}\hat{\Gamma}^P_{jj} - (\hat{\Gamma}^P)^2_{ij}}. \tag{98}$$

The thus derived mixing matrix elements include the full momentum dependence and imaginary parts of the Higgs boson self-energies. Therefore, the matrix is not unitary in general. Alternatively we could have set $k^2 = 0$ which corresponds to the result in the effective potential approximation and yields a unitary mixing matrix. For our parameter sets used in the numerical analysis we found that the differences in the two approaches are negligible. Furthermore, the imaginary parts of the mixing matrix elements are small compared to the real parts.

III. NUMERICAL ANALYSIS

The calculation of the Higgs and gauge boson self-energies, of the tadpoles and the counterterms has been performed numerically in two different calculations. In the first calculation all necessary Feynman rules have been derived from the NMSSM Lagrangian and implemented in a `FeynArts` model file [46]. In the second calculation the Feynman rules have been obtained with the Mathematica package `SARAH` [47]. The Feynman rules in the two approaches have been cross-checked against each other and also against the rules given in Ref. [8]. Subsequently, in both calculations `FormCalc` [48] was used to evaluate the self-energy and tadpole diagrams in the 't Hooft-Feynman gauge, in which the Goldstone bosons and the ghost fields have the same masses as the corresponding gauge bosons. The divergent integrals are regularized applying the constrained differential renormalization scheme [49] which has been shown to be equivalent [50] to the SUSY conserving dimensional reduction scheme [51]. The numerical computation of the integrals has been performed with `LoopTools` [48]. Two Mathematica programs have been written to evaluate the counterterms, diagonalize numerically the one-loop corrected Higgs boson mass matrices and extract the mass eigenvalues.

For our numerical analysis we follow the SUSY Les Houches Accord (SLHA) [52] and use as input values the Fermi constant $G_F = 1.16637 \times 10^{-5}$ GeV^{-2} and the Z boson mass $M_Z = 91.187$ GeV. For the electroweak coupling we set $\alpha = 1/137$. From these input values we derive the parameters of our input set defined in Eq. (29). The top quark pole mass is given by $M_t = 173.3$ GeV. As we cross-check our results against the ones of Ref. [41] which uses the running $\overline{\text{DR}}$ quark masses, we need to calculate these as well. In order to obtain the $\overline{\text{DR}}$ top quark mass we convert M_t at the scale $Q_t = M_t$ in the corresponding running mass. The SM renormalization group equations are then used to evolve the top mass up to a common scale Q chosen to be of the order of the SUSY breaking scale, where the gluino corrections are added. We denote the running top mass by m_t in the following. The same procedure is applied to the bottom mass starting from the SLHA input value $m_b(m_b)^{\overline{\text{MS}}}$ set equal to 4.19 GeV. The masses of the light quarks are chosen as $m_u = 2.5$ MeV, $m_c = 1.27$ GeV, $m_d = 4.95$ MeV, $m_s = 101$ MeV [53]. The τ mass has been set to $m_\tau = 1.777$ GeV.

In the following we will discuss the results for various scenarios which exemplify different effects of the higher-order corrections. For our scenarios, we took care not to violate unitarity bounds by choosing λ, κ such that $\sqrt{\lambda^2 + \kappa^2} \lesssim 0.7$. Furthermore, v_s has been chosen to be of the order of the vacuum expectation value v. As the one-loop corrections to the pseudoscalar masses are small, we mostly show plots for the scalar masses and comment

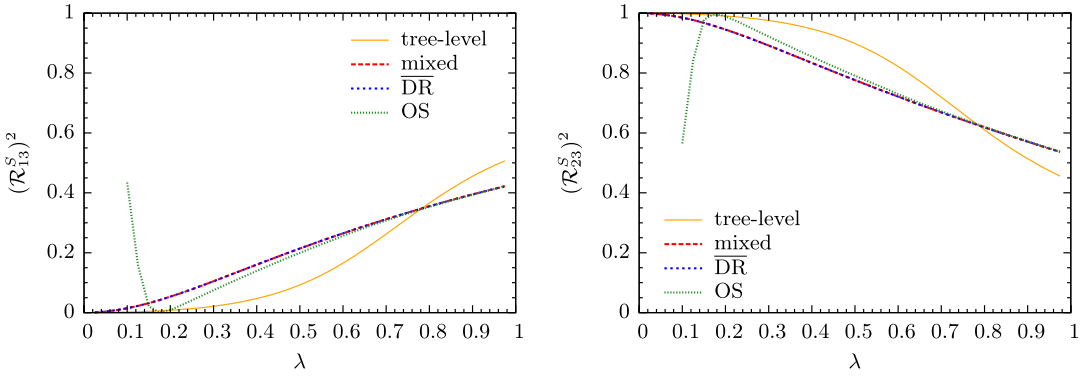

FIG. 1 (color online). The matrix element squared $(\mathcal{R}^S_{13})^2$ (left), $(\mathcal{R}^S_{23})^2$ (right) for the two lightest *CP*-even Higgs bosons as function of λ at tree-level (yellow/full) and at one-loop level adopting a $\overline{\text{DR}}$ (blue/dotted), a mixed (red/dashed) and an on-shell (green/small dotted) renormalization scheme.

briefly on the pseudoscalar masses. Furthermore, the corrections for the heaviest scalar Higgs boson are not shown, as in all cases they are negligible.

Variation of λ: We first verify that we reproduce the results of Ref. [41] by adopting a $\overline{\text{DR}}$ renormalization scheme and choosing the same parameter set

$$\kappa = \lambda/5, \qquad \tan\beta = 2, \qquad A_\lambda = 500 \text{ GeV}, \qquad A_\kappa = -10 \text{ GeV}, \qquad \mu = 250 \text{ GeV} \tag{99}$$

with λ being a free parameter and v_s given by $v_s = \sqrt{2}\mu/\lambda$. For the squarks and sleptons a common soft SUSY breaking mass $M_S = 300$ GeV has been adopted, and the remaining soft SUSY breaking parameters have been chosen as

$$A_t = A_b = A_\tau = -1.5 M_S, \qquad M_1 = M_S/3, \qquad M_2 = 2/3 M_S, \qquad M_3 = 2 M_S. \tag{100}$$

The renormalization scale has been set equal to $Q_0 = M_S$ and for the top and bottom quark mass the running $\overline{\text{DR}}$ mass at the scale Q_0 has been used. Furthermore, the light quark masses have been set to zero as in Ref. [41]. We find agreement for the one-loop corrected Higgs boson masses. Starting from this scenario in the $\overline{\text{DR}}$ scheme, in order to investigate the effect of different renormalization schemes, the $\overline{\text{DR}}$ input values have been converted to the mixed renormalization scheme as defined above, as well as to a pure on-shell scheme, and the Higgs boson masses and the matrix $\mathcal{R}^S$ are evaluated accordingly: With the SM parameters taken to be on-shell input values and the parameters in Eq. (99) taken to be $\overline{\text{DR}}$ input values all tree-level masses have been evaluated and were subsequently used to obtain the self-energies and counterterms. The thus calculated counterterms were used to convert the $\overline{\text{DR}}$ input values into on-shell input values and vice versa if needed. For the definitions of the schemes, see Subsec. II D. Using the scheme specific parameter sets, the tree-level Higgs masses needed in Eq. (87) were recalculated so that the one-loop Higgs masses could be obtained using the iterative procedure as described in Subsec. II E. In Fig. 1 we show the matrix elements squared $(\mathcal{R}^S_{13})^2$ and $(\mathcal{R}^S_{23})^2$, respectively, of the mixing matrix $\mathcal{R}^S$. These matrix elements are a measure of the strength of the singlet component of the two lightest Higgs bosons. They are shown for the three different renormalization schemes compared to the tree-level result as a function of λ. In order to match the result of Ref. [41] they have been evaluated at vanishing external momentum $k^2 = 0$. At tree-level, for small values of λ, the lightest *CP*-even Higgs boson is dominantly MSSM-like and the next-to-lightest is dominantly singletlike. With increasing λ the mixing increases and at tree-level there is a crossover at $\lambda \approx 0.94$: the next-to-lightest Higgs boson is now more MSSM-like than the lightest Higgs boson. The higher-order corrections change the amount of the singlet component and for this parameter set there is no crossover below $\lambda = 1$. Furthermore, we see that for $\lambda \gtrsim 0.2$ the amount of the singlet component is hardly affected by the renormalization scheme. The curves for the three renormalization schemes lie on top of each other for $\lambda \gtrsim 0.65$. For smaller values of λ, however, after having passed the values $(\mathcal{R}^S_{13})^2 = 0$ and $(\mathcal{R}^S_{23})^2 = 1$, respectively, $(\mathcal{R}^S_{13})^2$, $(\mathcal{R}^S_{23})^2$ in the OS-scheme start to differ largely from the corresponding values in the two other schemes. The reason is that the finite parts of the counterterms involved in the conversion from the $\overline{\text{DR}}$ parameters to on-shell parameters blow up in the limit $\lambda \to 0$. The H_1 mass squared even turns negative for $\lambda \lesssim 0.1$. The matrix elements and masses in the OS-scheme are therefore not plotted any more for λ values below this value.

Figure 2 shows the one-loop corrected mass M_{H_1} of the lightest (left) and M_{H_2} of the next-to-lightest (right) *CP*-even Higgs boson as a function of λ in the three different renormalization schemes compared to the tree-level result. The tree-level masses increase with rising λ due to the NMSSM contribution $\sim\lambda^2 \sin^2 2\beta$ from the Higgs quartic coupling. As H_1 is dominantly

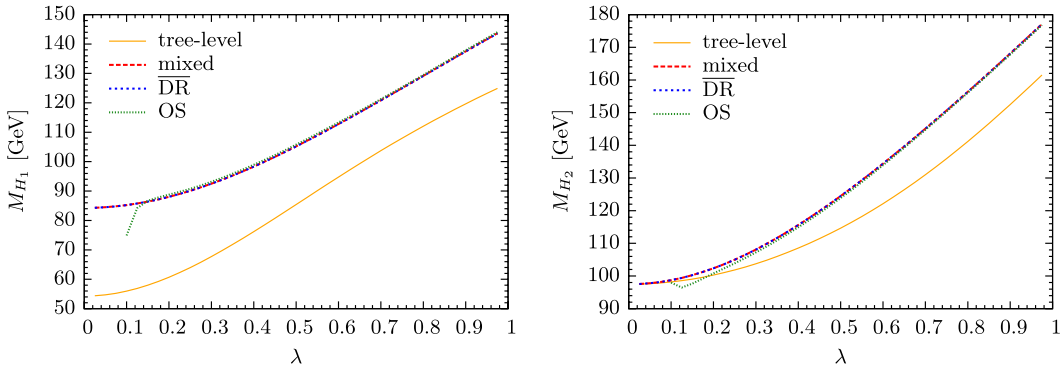

FIG. 2 (color online). The mass M_{H_1} of the lightest (left) and M_{H_2} of the next-to-lightest (right) CP-even Higgs boson as function of λ at tree-level (yellow/full) and at one-loop level adopting a $\overline{\text{DR}}$ (blue/dotted), a mixed (red/dashed) and an on-shell (green/small dotted) renormalization scheme.

MSSM-like its one-loop corrections are much more important than for the singlet dominated H_2. For the latter they are negligible at small λ and more important for large λ where H_2 is more MSSM-like. As can be inferred from the figures the deviations between the different schemes is negligible. The curves for all three schemes lie on top of each other, apart from small values of λ where the one-loop corrected H_1 and H_2 mass in the on-shell scheme start to differ from the $\overline{\text{DR}}$ and the mixed scheme.

The mass corrections and hence also the strengths of the singlet and MSSM component, respectively, strongly depend on the value of the top quark mass, which reflects the fact that the main part of the higher-order corrections stems from the top sector. Figure 3 shows the mixing matrix elements squared $(\mathcal{R}^S_{13})^2$, $(\mathcal{R}^S_{23})^2$ as functions of λ at one-loop level, calculated in the $\overline{\text{DR}}$ scheme, with the top quark mass taken as the running $\overline{\text{DR}}$ mass $m_t = 150.6$ GeV at the scale $Q_0 = 300$ GeV (including gluino effects) in one case and as the pole mass $M_t = 173.3$ GeV in the other case. For comparison the tree-level values are shown as well. Figure 4 displays the corresponding Higgs masses. In contrast to the case where the top quark mass has been set to the $\overline{\text{DR}}$ value, using the top pole mass leads to a one-loop corrected lightest Higgs boson which is singletlike and to a next-to-lightest Higgs boson being MSSM-like. Furthermore, the Higgs mass corrections are more important for a higher top quark mass value. Defining the relative correction $\Delta M_H/M_H$ as

$$\frac{\Delta M_H}{M_H} = \frac{|M_H - M_H^{(0)}|}{M_H^{(0)}}, \tag{101}$$

where M_H ($M_H^{(0)}$) denotes the 1-loop corrected (tree-level) Higgs boson mass, the relative correction for H_1 amounts to maximally 55% for the running mass and 79% for the pole mass. The large corrections also explain the change of the one-loop corrected H_1 from a MSSM-like to singletlike Higgs boson. In fact, due to the large corrections the one-loop corrected H_1 mass gets shifted above the one-loop corrected mass of H_2. Because of our convention to label by ascending indices the Higgs bosons with increasing mass, the H_1 one-loop corrected mass is assigned to H_2 and vice versa, so that H_1 and H_2 interchange their roles and H_1 becomes singletlike at 1-loop whereas H_2 becomes MSSM-like.

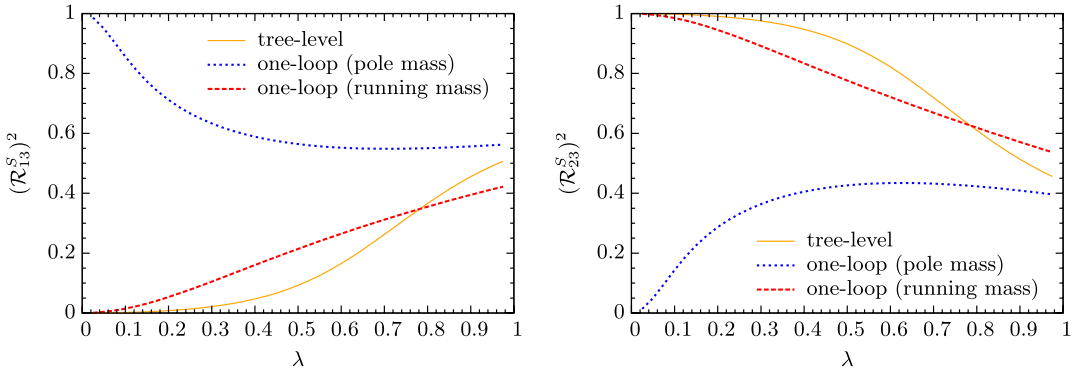

FIG. 3 (color online). The matrix element squared $(\mathcal{R}^S_{13})^2$ (left), $(\mathcal{R}^S_{23})^2$ (right) for the two lightest CP-even Higgs bosons as function of λ at tree-level (yellow/full), at one-loop level with the top quark pole mass (blue/dotted) and with the running $\overline{\text{DR}}$ top quark mass (red/dashed).

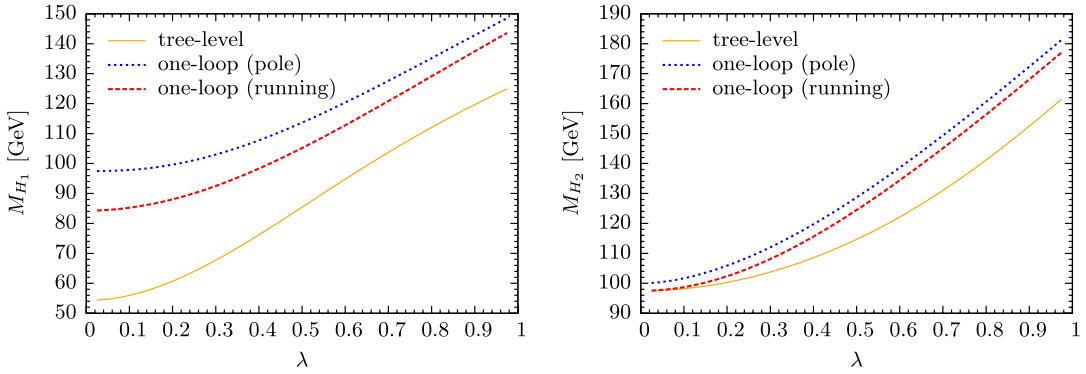

FIG. 4 (color online). The mass M_{H_1} of the lightest (left) and M_{H_2} of the next-to-lightest (right) *CP*-even Higgs boson as function of λ at tree-level (yellow/full), at one-loop level with the top quark pole mass (blue/dotted) and with the running $\overline{\text{DR}}$ top quark mass (red/dashed).

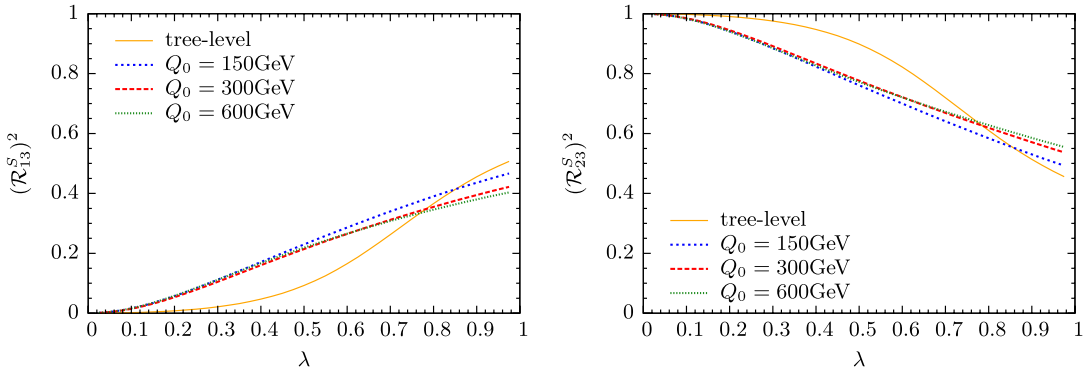

FIG. 5 (color online). The matrix element squared $(\mathcal{R}^S_{13})^2$ (left), $(\mathcal{R}^S_{23})^2$ (right) for the two lightest *CP*-even Higgs bosons as function of λ (taken at $Q_0 = 300$ GeV), at tree-level (yellow/full) and at one-loop level at the renormalization scale $Q_0 = 150$ GeV (blue/dotted), 300 GeV (red/dashed) and 600 GeV (green/small dotted).

In order to get an estimate of the missing higher-order corrections we investigate the influence of the renormalization scale Q_0. The results are shown (in the $\overline{\text{DR}}$ scheme) in Fig. 5 for the mixing matrix elements squared. They are plotted as a function of λ at tree-level and at one-loop level for three different values $Q_0 = 150$, 300 and 600 GeV. Note that the scale Q_0 also changes the value of the running b and t quark masses. In addition, the $\overline{\text{DR}}$ input values which are given at the scale of 300 GeV in Eq. (99) have to be converted to the respective Q_0. The corresponding plots for the masses of the two lightest Higgs bosons are depicted in Fig. 6. With rising Q_0 the running top quark mass decreases, leading to smaller one-loop Higgs boson mass corrections. The relative correction for the lightest Higgs boson mass is 62% for $Q_0 = 150$ GeV and 50% for $Q_0 = 600$ GeV. The relative correction of the next-to-lightest Higgs boson mass is changed less, with $\Delta M_{H_2}/M_{H_2} = 10\%$ and 12% for $Q_0 = 150$ and 600 GeV. This is due to the higher tree-level mass value. The residual theoretical uncertainties due to missing higher-order corrections can thus be estimated to $\mathcal{O}(10\%)$. These uncertainties as well as the dependence of the corrections on the value of top quark mass and/or the choice of the renormalization scheme, of course, get reduced once two-loop corrections are included in the calculation of the Higgs boson masses.

The amount of singlet component of the Higgs bosons strongly affects their couplings to fermions and gauge bosons and hence their phenomenology. In particular, with the small H_1 and H_2 mass values between ~90 and ~180 GeV, the question arises if the scenario has been excluded by LEP, Tevatron or LHC. We have explicitly verified that there are still regions in λ which have not been excluded. The allowed and excluded regions are shown in Fig. 7. The exclusion limit for $\lambda \leq 0.6$ where $M_{H_1} \lesssim 113$ GeV is due to the LEP exclusion[10] of M_{H_1} in the channel $e^+e^- \to ZH \to Zb\bar{b}$ [54]. The Tevatron [55] and the present LHC results [56,57] do not constrain the scenario. Note, that our limits represent a rough estimate

[10]The exclusion regions always apply to the one-loop corrected Higgs boson masses.

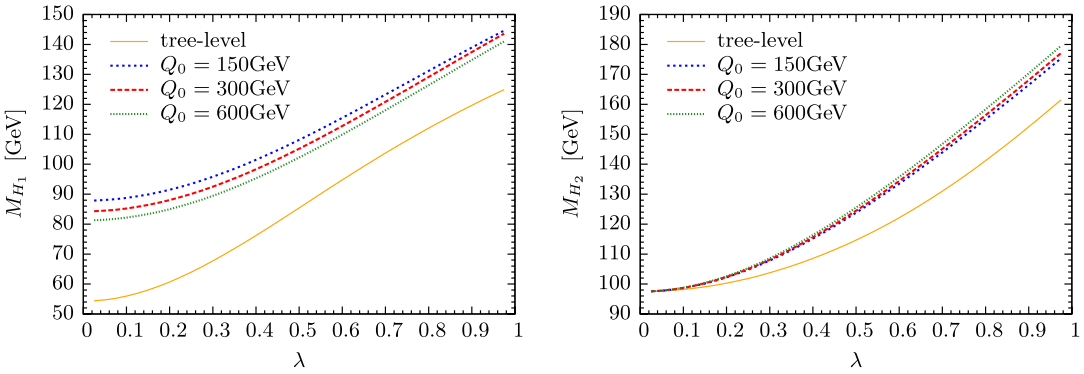

FIG. 6 (color online). The mass M_{H_1} of the lightest (left) and M_{H_2} of the next-to-lightest (right) CP-even Higgs boson as function of λ (taken at $Q_0 = 300$ GeV), at tree-level (yellow/full) and at one-loop level at the renormalization scale $Q_0 = 150$ GeV (blue/dotted), 300 GeV (red/dashed) and 600 GeV (green/small dotted).

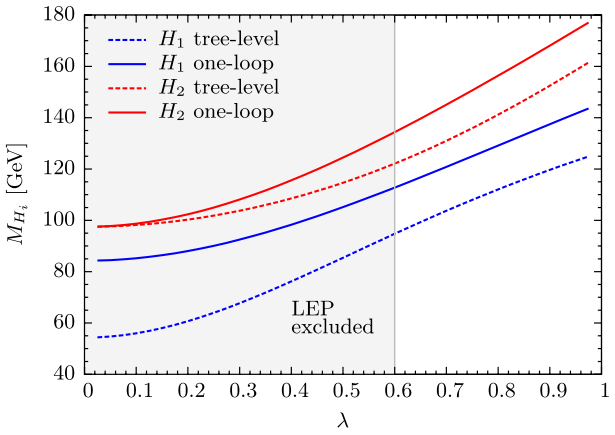

FIG. 7 (color online). The Higgs boson masses at tree-level (dashed) and one-loop (full) for H_1 (blue/dark grey) and H_2 (red/light grey) in the $\overline{\text{DR}}$ scheme with the exclusion limits set by LEP.

and cannot replace a sophisticated study of exclusion limits set by a combination of the experimental results. We have cross-checked though our exclusion limits against those obtained with `HiggsBounds` [58] and have found agreement.

Concerning the pseudoscalar Higgs bosons, the lighter state A_1 is singletlike, whereas the heavier one is MSSM-like, and the corrections are small. They are negative and in this scenario the relative corrections are below 2%. The masses increase with rising λ. The one-loop corrected mass M_{A_1} of the lighter pseudoscalar Higgs boson ranges between 40 and 140 GeV, and M_{A_2} takes values of 586 to 598 GeV.

Variation of A_κ: In the following the variation of the soft SUSY breaking coupling parameter A_κ is investigated. We have chosen a common soft SUSY breaking squark mass $m_0 = 1.1$ TeV and $M_S = 600$ GeV, large enough to fulfill the present exclusion limits on the squark masses of the first two generations and the gluino mass set by the LHC experiments [59]. The full parameter set is given by

$$\begin{aligned} &\lambda = 0.6, \quad \kappa = \lambda/3, \quad \tan\beta = 2, \quad A_\lambda = 500\,\text{GeV}, \\ &\mu = 275\,\text{GeV}, \quad A_t = A_b = A_\tau = -1.5 M_S, \\ &M_1 = M_S/3, \quad M_2 = 2/3 M_S, \quad M_3 = 2 M_S. \end{aligned} \tag{102}$$

The top and bottom quark masses have been chosen to be the pole masses, with $m_b^{\text{pole}} = 4.88$ GeV. The renormalization scheme is the mixed scheme as defined in Sec. II D and the input parameters are chosen accordingly. The renormalization scale has been set $Q_0 = 300$ GeV. The mixing matrix elements squared quantifying the amount of the singlet component of H_1 and H_2 are presented in Fig. 8 (left). They have been obtained by the procedure described in Sec. II E. We have explicitly verified that the difference to the values obtained by setting $k^2 = 0$ is negligible. The tree-level and one-loop corrected H_1 and H_2 masses are shown in Fig. 8 (right). As can be inferred from the figure, for large negative values of A_κ the lightest Higgs boson is mostly singletlike and the heavier one MSSM-like. With increasing A_κ the mixing increases developing a rapid crossover at $A_\kappa \approx -294$ GeV. The one-loop corrections shift the crossover to a larger value $A_\kappa \approx -240$ GeV. This behavior is also reflected in the Higgs boson masses. Below (above) the crossover the lightest (next-to-lightest) Higgs boson is mostly singletlike and exhibits a strong dependence on A_κ, whereas in the MSSM-like case the Higgs bosons hardly depend on A_κ. This behavior results from the fact that the soft SUSY breaking term which contains A_κ is a cubic coupling in the singlet field S. A variation of A_κ can hence only be communicated through a singlet contribution of the Higgs boson fields. Since the mixing is small, only fields which are mainly singletlike are affected. Despite the singlet character of H_1 for small A_κ the one-loop corrections can be important and more than triple the mass. This is mainly due to the small tree-level value. In case of the next-to-lightest Higgs boson H_2 the one-loop corrections in the singletlike case are less pronounced and of $\mathcal{O}(10\,\text{GeV})$. The corrections to the

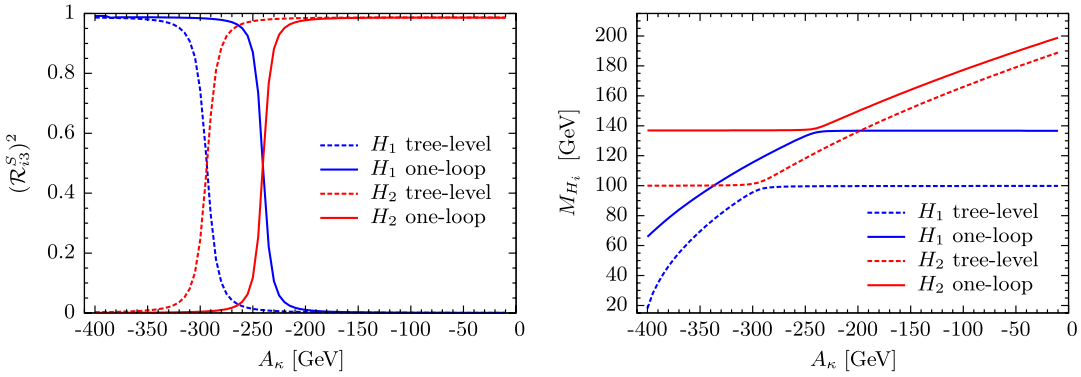

FIG. 8 (color online). Left: The matrix elements squared $(\mathcal{R}^S_{i3})^2$ $(i = 1, 2)$ as function of A_κ at tree-level (dashed) and one-loop (full) for H_1 (blue/dark grey) and H_2 (red/light grey). Right: The corresponding tree-level and one-loop corrected masses.

MSSM-like Higgs bosons increase the masses by about 37 GeV. No Higgs boson mass values $M_{H_{1,2}}$ have been excluded so far by the experiments. With a slightly higher value of λ, however, the MSSM-like Higgs boson mass gets shifted above 141 GeV, so that the scenario would be excluded by the new LHC exclusion limits [57].

For the pseudoscalar masses the relative corrections are very small, at the 6% level for the singletlike A_1 and below 0.2% for the heavier A_2. The one-loop masses decrease with decreasing absolute value of A_κ and are 110 GeV $\lesssim M_{A_1} \lesssim$ 345 GeV and 639 GeV $\lesssim M_{A_2} \lesssim$ 640 GeV for $0\,\text{GeV} \geq A_\kappa \geq -400$ GeV.

Variation of $M_{H^\pm}$: Here, we present results for a variation of the charged Higgs boson mass, *cf.* Eq. (14). The other parameters are kept fixed and chosen as

$$\begin{aligned} &\lambda = 0.65, \quad \kappa = \lambda/3, \quad \tan\beta = 2, \quad A_\kappa = -10\,\text{GeV}, \\ &\mu = 225\,\text{GeV}, \quad A_t = A_b = A_\tau = -1.5 M_S, \\ &M_1 = M_S/3, \quad M_2 = 2/3 M_S, \quad M_3 = 2 M_S. \end{aligned} \tag{103}$$

The common soft SUSY breaking squark mass is once again taken to be $m_0 = 1.1\,\text{TeV}$ and $M_S = 600$ GeV. Note, that the input parameters are defined according to the mixed renormalization scheme and the renormalization scale $Q_0 = 300$ GeV. The charged Higgs mass is varied between $M_{H^\pm} \approx 420 \ldots 610$ GeV. Outside this parameter range the H_1 mass squared becomes negative.[11] The results for the singlet components and Higgs boson masses at tree-level and one-loop are shown in Fig. 9. The lightest Higgs boson H_1 is dominantly MSSM-like with a 100% MSSM component at $M_{H^\pm} \approx 520$ GeV. Here H_2 is maximally singletlike, though not completely. The heaviest scalar Higgs boson H_3 takes over the remaining singlet component (not shown here), so that $\sum_{i=1\ldots3}(\mathcal{R}^S_{i3})^2 = 1$ as demanded by unitarity of the mixing matrix.[12] The one-loop corrections increase the mixing between H_1 and H_2 away from the maximum and minimum singlet values. They lead to a more pronounced maximum and minimum in the singlet component and slightly shift their positions to smaller $H^\pm$ masses, $M_{H^\pm} \approx 518$ GeV. The H_1 and H_2 masses are maximal and minimal, respectively, at the position of minimal mixing. Because of its MSSM nature the lightest Higgs boson receives large one-loop corrections. The correction is $\sim$35 GeV for M_{H_1} at its maximum value, which is taken at $M_{H^\pm} \approx 515$ GeV, and can even triple the tree-level mass at the borders of the $M_{H^\pm}$ range. The latter is mostly the effect of an already very small tree-level mass of $\sim$30 GeV. The singletlike H_2 on the other hand receives smaller corrections which can nevertheless reach 10 GeV. The investigated parameter range has been partially excluded as indicated in Fig. 9 (right). For $M_{H^\pm} \leq$ 452 GeV light Higgs boson masses $M_{H_1} \lesssim 112$ GeV have been excluded by the LEP searches in $ZH \to Zb\bar{b}$ [54]. The right exclusion limit $M_{H^\pm} \geq 585$ GeV is also due to the LEP exclusion of $M_{H_1} \lesssim 113.5$ GeV in the $ZH \to Zb\bar{b}$ channel. The Tevatron results do not exclude Higgs mass values. The exclusion limits obtained with HIGGSBOUNDS agree with ours. The maximum mass value taken by the MSSM-like lightest scalar Higgs boson is 140.5 GeV. It is just below the value excluded by the newest LHC limits [57]. In view of the uncertainties associated with the 1-loop Higgs mass corrections and also taking into account the fact that our exclusion limits are only a rough estimate, the scenario might be excluded for charged Higgs mass values around 515 GeV.

The influence of the renormalization scheme on the one-loop corrected $H_{1,2}$ masses is shown in Fig. 10. They are

[11] See also Ref. [42] for a discussion of the Higgs boson masses and their dependence on the NMSSM parameters.

[12] It should be noted that this is only approximately true for the matrix obtained via the procedure described in Sect. II E. In general this matrix, in contrast to the one obtained using $k^2 = 0$, is not unitary. As already mentioned the difference between the two approaches is small for our scenarios.

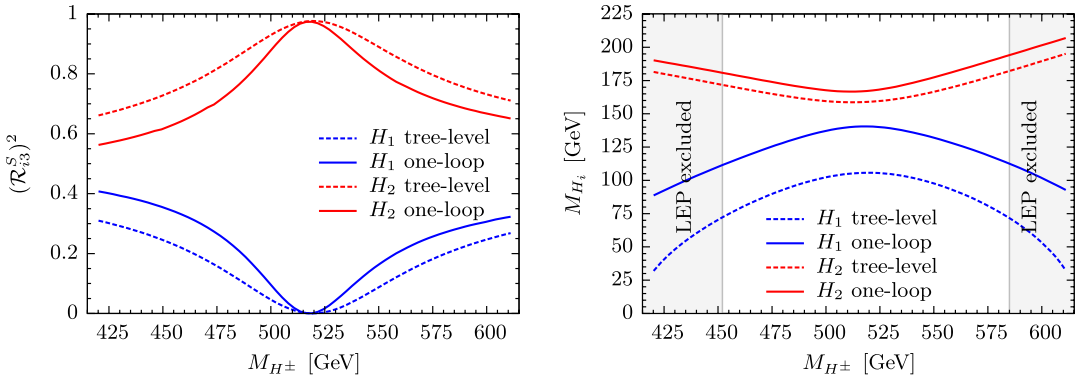

FIG. 9 (color online). Left: The matrix elements squared $(\mathcal{R}^S_{i3})^2$ $(i = 1, 2)$ as function of $M_{H^\pm}$ at tree-level (dashed) and one-loop (full) for H_1 (blue/dark grey) and H_2 (red/light grey). Right: The corresponding tree-level and one-loop corrected masses with the exclusion limits.

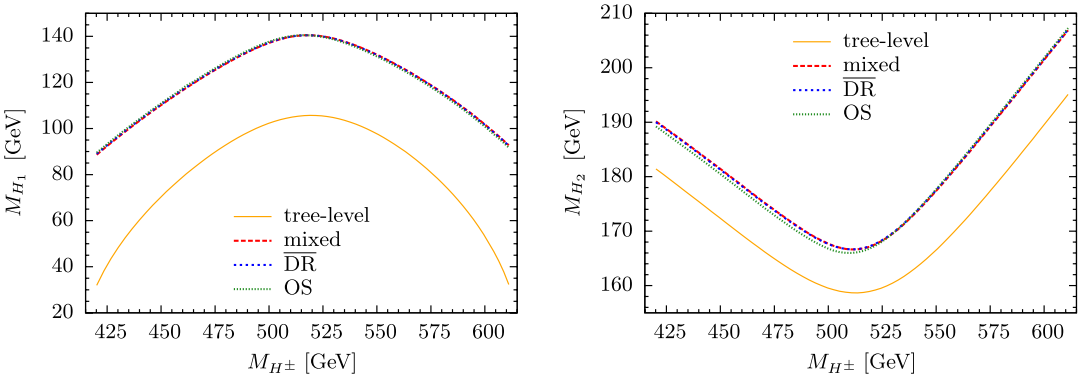

FIG. 10 (color online). The mass M_{H_1} of the lightest (left) and M_{H_2} of the next-to-lightest (right) CP-even Higgs boson as function of $M_{H^\pm}$ at tree-level (yellow/full) and at one-loop level adopting a $\overline{\text{DR}}$ (blue/dotted), a mixed (red/dashed) and an on-shell (green/small dotted) renormalization scheme.

shown as functions of $M_{H^\pm}$ in the OS, mixed and pure $\overline{\text{DR}}$ scheme and compared to the tree-level result. For the OS and pure $\overline{\text{DR}}$ scheme the input values, which are defined in the mixed scheme, are then converted to the corresponding scheme where necessary. For the chosen parameter set the results of the three different approaches show only minor differences.

In Fig. 11 we show the tree-level and one-loop corrected masses of the pseudoscalar Higgs bosons as functions of $M_{H^\pm}$. Whereas for the heavier CP-odd boson the

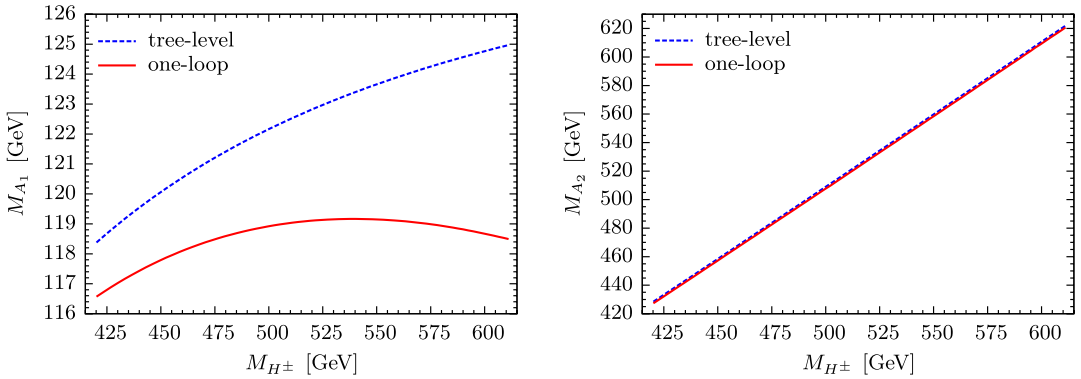

FIG. 11 (color online). The mass M_{A_1} of the lighter (left) and M_{A_2} of the heavier (right) pseudoscalar Higgs boson as a function of $M_{H^\pm}$ at tree-level (dashed/blue) and at one-loop (full/red).

corrections are negligible they can be of $\mathcal{O}(5\%)$ for the lighter one at large values of $M_{H^\pm}$. Nevertheless they are much smaller than the corrections for the lightest scalar Higgs boson.

IV. SUMMARY AND CONCLUSIONS

In summary, we have calculated the one-loop corrections to the NMSSM Higgs masses in a renormalization scheme which mixes on-shell and $\overline{\text{DR}}$ conditions, by applying the latter solely to the parameters $\tan\beta$, v_s, λ, κ, A_κ. We have compared our result to a pure $\overline{\text{DR}}$ and a pure OS-scheme. Apart from special parameter regions which unphysically blow up the counterterms, there is hardly any difference in the results for the masses of the NMSSM Higgs bosons in the three different renormalization schemes. Another estimate of the effect of the missing higher-order corrections is given by the variation of the renormalization scale. We found the effect on the Higgs mass corrections to be $\mathcal{O}(10\%)$ or less. The bulk of the one-loop corrections stems from the top quark sector as is known from the MSSM. This is reflected in the difference of the relative corrections for the lightest Higgs boson mass. The relative correction in the scenario, which we investigated, is equal to 55% when adopting the running $\overline{\text{DR}}$ mass and 79% in case of the top quark pole mass. The theoretical uncertainty estimated from the effects originating from the top sector is hence $\mathcal{O}(10\%)$. These effects are reduced significantly of course once the known two-loop corrections are included. Furthermore, the higher-order corrections can shift the point of crossover between singletlike and MSSM-like behavior of the Higgs bosons. This dictates also the amount of coupling to the gauge bosons and fermions and hence influences the Higgs boson phenomenology. The precise knowledge of the higher-order corrections is therefore indispensable for a proper investigation of specific production and decay scenarios and a proper interpretation of the experimental results.

ACKNOWLEDGMENTS

This research was supported in part by the Deutsche Forschungsgemeinschaft via the Sonderforschungsbereich/Transregio SFB/TR-9 Computational Particle Physics. Part of this work has been performed while T. G. has been at the Institut für Theoretische Physik, Karlsruhe Institute of Technology, as well as while H. R. has been at Physikalisches Institut, Albert-Ludwigs-Universität Freiburg.

APPENDIX A: THE *CP*-EVEN AND *CP*-ODD MASS MATRICES

In the following we display the mass matrices in terms of the parameters for which we apply our renormalization conditions. We repeat them here for completeness, *cf.* also Eq. (29),

$$t_{h_u},\ t_{h_d},\ t_{h_s},\ e,\ M_W^2,\ M_Z^2,\ \tan\beta,\ M_{H^\pm}^2,\ \lambda,\ \kappa,\ v_s,\ A_\kappa. \tag{A1}$$

Note, that in the mass matrices we paid attention to keep the distinction in the angle β and the angle β_B. The difference of these two angles is denoted as

$$\Delta\beta = \beta - \beta_B. \tag{A2}$$

Here, β is defined by the ratio of the vacuum expectation values of the neutral components of the two Higgs doublets H_u and H_d, $\tan\beta = v_u/v_d$. The angle β_B on the other hand performs the rotation from the basis (a_d, a_u, a_s) to the basis (a, a_s, G) to separate a massless Goldstone boson. It is the angle β which receives a counterterm. The angle β_B also enters the scalar mass matrix. This is due to the replacement Eq. (27) of A_λ in terms of the parameter set Eq. (A1).

The scalar 3×3 mass matrix M_S^2 in the basis $h^S = (h_d, h_u, h_s)^T$ is given by the entries $M_{S_{ij}}^2 = M_{S_{ji}}^2$ $(i, j = 1, 2, 3)$, with

$$\begin{aligned} M_{S_{11}}^2 = {} & \frac{e c_\beta c_{\beta_B}^2}{2 M_W s_W c_{\Delta\beta}^2}[t_{h_d}(2 t_\beta t_{\beta_B} + 1) - t_{h_u} t_\beta] \\ & + \frac{s_\beta^2}{c_{\Delta\beta}^2}[M_{H^\pm}^2 + (M_Z^2 t_\beta^{-2} - M_W^2) c_{\Delta\beta}^2] \\ & + \frac{2\lambda^2 M_W^2 s_W^2 s_\beta^2}{e^2} \end{aligned} \tag{A3}$$

$$\begin{aligned} M_{S_{12}}^2 = {} & \frac{e c_\beta c_{\beta_B}^2}{2 M_W s_W c_{\Delta\beta}^2}[t_{h_d} t_\beta t_{\beta_B}^2 + t_{h_u}] \\ & - \frac{s_\beta c_\beta}{c_{\Delta\beta}^2}[M_{H^\pm}^2 + (M_Z^2 - M_W^2) c_{\Delta\beta}^2] + \frac{\lambda^2 M_W^2 s_W^2 s_{2\beta}}{e^2} \end{aligned} \tag{A4}$$

$$M_{S_{13}}^2 = \frac{s_\beta c_\beta c_{\beta_B}^2}{v_s c_{\Delta\beta}^2}[t_{h_d} t_\beta t_{\beta_B}^2 + t_{h_u}] + \frac{2 M_W s_W s_\beta^2 c_\beta}{e v_s c_{\Delta\beta}^2}[M_W^2 c_{\Delta\beta}^2 - M_{H^\pm}^2] + \frac{\lambda M_W s_W c_\beta v_s}{e}[2\lambda - \kappa t_\beta] + \frac{-4\lambda^2 M_W^3 s_W^3 s_\beta^2 c_\beta}{e^3 v_s} \tag{A5}$$

$$M_{S_{22}}^2 = \frac{e c_\beta c_{\beta_B}}{2 M_W s_W c_{\Delta\beta}^2}[-t_{h_d} s_{\beta_B} t_{\beta_B} + t_{h_u} s_{\beta_B}(t_\beta t_{\beta_B} + 2)] + \frac{c_\beta^2}{c_{\Delta\beta}^2}[M_{H^\pm}^2 + (M_Z^2 t_\beta^2 - M_W^2) c_{\Delta\beta}^2] + \frac{2\lambda^2 M_W^2 s_W^2 c_\beta^2}{e^2} \tag{A6}$$

$$M^2_{S_{23}} = \frac{c^2_\beta c^2_{\beta_B}}{v_s c^2_{\Delta\beta}}[t_{h_d} t_\beta t^2_{\beta_B} + t_{h_u}] + \frac{2M_W s_W s_\beta c^2_\beta}{e v_s c^2_{\Delta\beta}}[M^2_W c^2_{\Delta\beta} - M^2_{H^\pm}] + \frac{\lambda M_W s_W c_\beta v_s}{e}[2\lambda t_\beta - \kappa] + \frac{-4\lambda^2 M^3_W s^3_W s_\beta c^2_\beta}{e^3 v_s} \quad \text{(A7)}$$

$$M^2_{S_{33}} = \kappa A_\kappa \frac{v_s}{\sqrt{2}} + 2\kappa^2 v_s^2 + \frac{t_{h_s}}{v_s} + \frac{2M_W s_W s_\beta c^2_\beta}{e^2 v_s^2 c^2_{\Delta\beta}}[2M^2_{H^\pm} M_W s_W s_\beta - e(t_{h_d} t_\beta s^2_{\beta_B} + t_{h_u} c^2_{\beta_B})]$$
$$+ \frac{M^2_W s^2_W s_{2\beta}}{e^4 v_s^2}[2\lambda^2 M^2_W s^2_W s_{2\beta} - \kappa\lambda e^2 v_s^2 - M^2_W e^2 s_{2\beta}]. \quad \text{(A8)}$$

We have introduced here the shortcuts $c_W \equiv \cos\theta_W = M_W/M_Z$ and $s_W \equiv \sin\theta_W$. The entries $M^2_{P_{ij}} = M^2_{P_{ji}}$ $(i, j = 1, 2, 3)$ of the pseudoscalar 3×3 mass matrix M^2_P in the basis $h^P = (a, a_s, G)^T$ read

$$M^2_{P_{11}} = \frac{2\lambda^2 M^2_W s^2_W c^2_{\Delta\beta}}{e^2} + M^2_{H^\pm} - M^2_W c^2_{\Delta\beta} \quad \text{(A9)}$$

$$M^2_{P_{12}} = \frac{M_W s_W s_{2\beta}}{e v_s c_{\Delta\beta}}[M^2_{H^\pm} - M^2_W c^2_{\Delta\beta}] - \frac{c_\beta c^2_{\beta_B}}{v_s c_{\Delta\beta}}[t_{h_u} + t_{h_d} t_\beta t^2_{\beta_B}] + \frac{\lambda M_W s_W c_{\Delta\beta}}{e^3 v_s}[2\lambda M^2_W s^2_W s_{2\beta} - 3\kappa e^2 v_s^2] \quad \text{(A10)}$$

$$M^2_{P_{13}} = M^2_{H^\pm} t_{\Delta\beta} + \frac{M^2_W s_{2\Delta\beta}}{2e^2}[2\lambda^2 s^2_W - e^2] + \frac{e c_{\beta_B}}{2M_W s_W c_{\Delta\beta}}[t_{h_d} t_{\beta_B} - t_{h_u}] \quad \text{(A11)}$$

$$M^2_{P_{22}} = -3A_\kappa \kappa \frac{v_s}{\sqrt{2}} + \frac{t_{h_s}}{v_s} - \frac{2M_W s_W s_\beta c^2_\beta c^2_{\beta_B}}{e v_s^2 c^2_{\Delta\beta}}[t_{h_u} + t_{h_d} t_\beta t^2_{\beta_B}] + \frac{M^2_W s^2_W s^2_{2\beta}}{e v_s^2 c^2_{\Delta\beta}}[M^2_{H^\pm} - M^2_W c^2_{\Delta\beta}]$$
$$+ \frac{\lambda M^2_W s^2_W s_{2\beta}}{e^4 v_s^2}[2\lambda M^2_W s^2_W s_{2\beta} + 3\kappa e^2 v_s^2] \quad \text{(A12)}$$

$$M^2_{P_{23}} = \frac{M_W s_W s_{2\beta}}{2e v_s c_{\Delta\beta}}[2M^2_{H^\pm} t_{\Delta\beta} - M^2_W s_{2\Delta\beta}] - \frac{c_\beta c^2_{\beta_B} t_{\Delta\beta}}{v_s c_{\Delta\beta}}[t_{h_u} + t_{h_d} t_\beta t^2_{\beta_B}] + \frac{\lambda M_W s_W s_{\Delta\beta}}{e^3 v_s}[2\lambda M^2_W s^2_W s_{2\beta} - 3\kappa e^2 v_s^2] \quad \text{(A13)}$$

$$M^2_{P_{33}} = M^2_{H^\pm} \tan^2\Delta\beta + \frac{M^2_W \sin^2\Delta\beta}{e^2}[2\lambda^2 s^2_W - e^2] + \frac{e}{2M_W s_W c^2_{\Delta\beta}}[t_{h_d} c_{\beta - 2\beta_B} - t_{h_u} s_{\beta - 2\beta_B}]. \quad \text{(A14)}$$

APPENDIX B: FERMIONIC SELF-ENERGIES

In this Appendix we give the renormalized fermionic self-energies which are needed in the determination of the counterterms δv_s and $\delta\kappa$ from the chargino and the neutralino sector, respectively. We start from the general structure of a fermionic self-energy given by Eq. (60), which also applies to the corresponding renormalized self-energies. The left- and right-chiral chargino fields $\psi^\pm_{L,R}$ in the interaction basis are given in terms of the Weyl spinors for the gaugino fields $\tilde{W}_1, \tilde{W}_2$ and the charged components of the higgsino fields $\tilde{H}^\pm_d, \tilde{H}^\pm_u$,

$$\psi^-_R = \begin{pmatrix} \tilde{W}^- \\ \tilde{H}^-_d \end{pmatrix}, \qquad \psi^+_L = \begin{pmatrix} \tilde{W}^+ \\ \tilde{H}^+_u \end{pmatrix}, \quad \text{(B1)}$$

with $\tilde{W}^\pm = (\tilde{W}_1 \mp i\tilde{W}_2)/\sqrt{2}$. The chargino fields in the interaction basis are replaced by the renormalized fields and the corresponding field renormalization constants,

$$\psi^\pm_{L,R} \to \left(\mathbb{1} + \frac{1}{2}\delta Z_{L,R}\right)\psi^\pm_{L,R}, \quad \text{with}$$
$$\delta Z_{L,R} = \begin{pmatrix} \delta Z_{L_1,R_1} & 0 \\ 0 & \delta Z_{L_2,R_2} \end{pmatrix}, \quad \text{(B2)}$$

and the 2×2 chargino mass matrix by

$$M_C \to M_C + \delta(M_C). \quad \text{(B3)}$$

Performing the rotation of $\psi^\pm_{L,R}$ to the fields $\chi^\pm_{L,R}$ in the mass eigenbasis with the unitary matrices U and V,

$$\chi^+_L = V\psi^+_L, \qquad \chi^-_R = U\psi^-_R, \quad \text{(B4)}$$

yields for the renormalized self-energies $\hat{\Sigma}$ in the mass eigenbasis in terms of the unrenormalized self-energies,

field renormalization constants and mass matrix counterterm

$$\hat{\Sigma}^{R}_{\chi^{\pm}}(k^2) = \Sigma^{R}_{\chi^{\pm}}(k^2) + \frac{1}{2}U^*(\delta Z_R + \delta Z_R^*)U^T \tag{B5}$$

$$\hat{\Sigma}^{L}_{\chi^{\pm}}(k^2) = \Sigma^{L}_{\chi^{\pm}}(k^2) + \frac{1}{2}V(\delta Z_L + \delta Z_L^*)V^\dagger \tag{B6}$$

$$\hat{\Sigma}^{Ls}_{\chi^{\pm}}(k^2) = \Sigma^{Ls}_{\chi^{\pm}}(k^2) - \frac{1}{2}U^*(\delta Z_R M_C + M_C \delta Z_L)V^\dagger - U^*\delta(M_C)V^\dagger \tag{B7}$$

$$\hat{\Sigma}^{Rs}_{\chi^{\pm}}(k^2) = \Sigma^{Rs}_{\chi^{\pm}}(k^2) - \frac{1}{2}V(\delta Z_L^* M_C^\dagger + M_C^\dagger \delta Z_R^*)U^T - V\delta(M_C^\dagger)U^T. \tag{B8}$$

The self-energies are 2×2 matrices. The corresponding renormalized self-energies in the neutralino sector, which are 5×5 matrices, are obtained analogously and read

$$\hat{\Sigma}^{R}_{\chi^0}(k^2) = \Sigma^{R}_{\chi^0}(k^2) + \frac{1}{2}\mathcal{N}^*(\delta Z_R + \delta Z_R^*)\mathcal{N}^T \tag{B9}$$

$$\hat{\Sigma}^{L}_{\chi^0}(k^2) = \Sigma^{L}_{\chi^0}(k^2) + \frac{1}{2}\mathcal{N}(\delta Z_L + \delta Z_L^*)\mathcal{N}^\dagger \tag{B10}$$

$$\hat{\Sigma}^{Ls}_{\chi^0}(k^2) = \Sigma^{Ls}_{\chi^0}(k^2) - \frac{1}{2}\mathcal{N}^*(\delta Z_R M_N + M_N \delta Z_L)\mathcal{N}^\dagger - \mathcal{N}^*\delta(M_N)\mathcal{N}^\dagger \tag{B11}$$

$$\hat{\Sigma}^{Rs}_{\chi^0}(k^2) = \Sigma^{Rs}_{\chi^0}(k^2) - \frac{1}{2}\mathcal{N}(\delta Z_L^* M_N^\dagger + M_N^\dagger \delta Z_R^*)\mathcal{N}^T - \mathcal{N}\delta(M_N^\dagger)\mathcal{N}^T, \tag{B12}$$

where $\mathcal{N}$ is the unitary 5×5 matrix which performs the rotation from the interaction basis to the neutralino mass eigenbasis. Allowing also for negative neutralino mass values, as we do, the matrix is real. The neutralino mass matrix M_N is given in Eq. (19) and $\delta Z_{L,R}$ denote diagonal 5×5 matrices with the field renormalization constants in the interaction eigenbasis,[13] $\delta Z_{L_i,R_i}$ $(i = 1, \ldots, 5)$, as entries. Note that δZ_L and δZ_R are related due to the Majorana character of the neutralinos.

[13]For better readability we did not choose a different notation for the field renormalization constants in the chargino and the neutralino case. They are understood to be different, though.

[1] D. V. Volkov and V. P. Alkulov, Phys. Lett. B **46**, 109 (1973); J. Wess and B. Zumino, Nucl. Phys. **B70**, 39 (1974); P. Fayet, Phys. Lett. B **64**, 159 (1976); **69**, 489 (1977); **84**, 416 (1979); G. F. Farrar and P. Fayet, Phys. Lett. B **76**, 575 (1978); E. Witten, Nucl. Phys. **B188**, 513 (1981); H. P. Nilles, Phys. Rep. **110**, 1 (1984); H. E. Haber and G. L. Kane, Phys. Rep. **117**, 75 (1985); M. F. Sohnius, Phys. Rep. **128**, 39 (1985); J. F. Gunion and H. E. Haber, Nucl. Phys. **B272**, 1 (1986); **B402**, 567 (1993); **B278**, 449 (1986); A. B. Lahanas and D. V. Nanopoulos, Phys. Rep. **145**, 1 (1987).

[2] S. Dimopoulos and H. Georgi, Nucl. Phys. **B193**, 150 (1981); N. Sakai, Z. Phys. C **11**, 153 (1981).

[3] E. Witten, Phys. Lett. B **105**, 267 (1981); S. Dimopoulos and H. Georgi, Nucl. Phys. **B193**, 150 (1981); J. Polchinski and L. Susskind, Phys. Rev. D **26**, 3661 (1982); R. K. Kaul and P. Majumdar, Nucl. Phys. **B199**, 36 (1982).

[4] For reviews and further references, see: J. F. Gunion, H. E. Haber, G. Kane, and S. Dawson, *The Higgs Hunter's Guide* (Addison-Wesley, Reading, MA, 1990); S. P. Martin, arXiv:hep-ph/9709356; S. Dawson, arXiv:hep-ph/9712464; M. Gomez-Bock, M. Mondragon, M. Mühlleitner, R. Noriega-Papaqui, I. Pedraza, M. Spira, and P. M. Zerwas, J. Phys. Conf. Ser. **18**, 74 (2005); M. Gomez-Bock, M. Mondragon, M. Mühlleitner, M. Spira, and P. M. Zerwas, arXiv:0712.2419; A. Djouadi, Phys. Rep. **459**, 1 (2008).

[5] J. E. Kim and H. P. Nilles, Phys. Lett. B **138**, 150 (1984).

[6] P. Fayet, Nucl. Phys. **B90**, 104 (1975); R. Barbieri, S. Ferrara, and C. A. Savoy, Phys. Lett. B **119**, 343 (1982); M. Dine, W. Fischler, and M. Srednicki, Phys. Lett. B **104**, 199 (1981); H. P. Nilles, M. Srednicki, and D. Wyler, Phys. Lett. B **120**, 346 (1983); J. M. Frere, D. R. T. Jones, and S. Raby, Nucl. Phys. **B222**, 11 (1983); J. P. Derendinger and C. A. Savoy, Nucl. Phys. **B237**, 307 (1984).

[7] J. R. Ellis, J. F. Gunion, H. E. Haber, L. Roszkowski, and F. Zwirner, Phys. Rev. D **39**, 844 (1989); M. Drees, Int. J. Mod. Phys. A **4**, 3635 (1989); U. Ellwanger, M. Rausch de Traubenberg, and C. A. Savoy, Phys. Lett. B **315**, 331 (1993); Z. Phys. C **67**, 665 (1995); Nucl. Phys. **B492**, 21 (1997); T. Elliott, S. F. King, and P. L. White, Phys. Lett. B **351**, 213 (1995); S. F. King and P. L. White, Phys. Rev. D **52**, 4183 (1995); F. Franke and H. Fraas, Int. J. Mod. Phys. A **12**, 479 (1997).

[8] For a review see, M. Maniatis, Int. J. Mod. Phys. A **25**, 3505 (2010).

[9] For a review see, U. Ellwanger, C. Hugonie, and A. M. Teixeira, Phys. Rep. **496**, 1 (2010).

[10] R. Barate *et al.* (LEP Working Group for Higgs boson searches, ALEPH, DELPHI, L3, and OPAL Collaborations), Phys. Lett. B **565**, 61 (2003); S. Schael *et al.* (ALEPH, DELPHI, L3, OPAL, and LEP Working Group for Higgs Boson Searches Collaborations), Eur. Phys. J. C **47**, 547 (2006).

[11] U. Ellwanger, J. F. Gunion, C. Hugonie, and S. Moretti, arXiv:hep-ph/0305109; arXiv:hep-ph/0401228; U. Ellwanger, J. F. Gunion, and C. Hugonie, J. High Energy Phys. 07 (2005) 041; S. Moretti, S. Munir, and P. Poulose, Phys. Lett. B **644**, 241 (2007); T. Stelzer, S. Wiesenfeldt, and S. Willenbrock, Phys. Rev. D **75**, 077701 (2007); K. Cheung, J. Song, and Q.-S. Yan, Phys. Rev. Lett. **99**, 031801 (2007); M. Carena, T. Han, G.-Y. Huang, and C. E. M. Wagner, J. High Energy Phys. 04 (2008) 092; J. R. Forshaw, J. F. Gunion, L. Hodgkinson, A. Papaefstathiou, and A. D. Pilkington, J. High Energy Phys. 04 (2008) 090; A. Djouadi, M. Drees, U. Ellwanger, R. Godbole, C. Hugonie, S. F. King, S. Lehti, and S. Moretti *et al.*, J. High Energy Phys. 07 (2008) 002; A. Djouadi, U. Ellwanger, and A. M. Teixeira, J. High Energy Phys. 04 (2009) 031; F. Mahmoudi, J. Rathsman, O. Stal, and L. Zeune, Eur. Phys. J. C **71**, 1608 (2011); O. Stal and G. Weiglein, J. High Energy Phys. 01 (2012) 071; M. M. Almarashi and S. Moretti, Phys. Rev. D **85**, 017701 (2012).

[12] R. Dermisek and J. F. Gunion, Phys. Rev. Lett. **95**, 041801 (2005); Phys. Rev. D **73**, 111701 (2006); Phys. Rev. D **75**, 075019 (2007); Phys. Rev. D **76**, 095006 (2007).

[13] Y. Okada, M. Yamaguchi, and T. Yanagida, Prog. Theor. Phys. **85**, 1 (1991); Phys. Lett. B **262**, 54 (1991); J. R. Ellis (CERN), G. Ridolfi, and F. Zwirner, Phys. Lett. B **257**, 83 (1991); Phys. Lett. B **262**, 477 (1991); H. E. Haber and R. Hempfling, Phys. Rev. Lett. **66**, 1815 (1991).

[14] P. H. Chankowski, S. Pokorski, and J. Rosiek, Phys. Lett. B **274**, 191 (1992); Nucl. Phys. **B423**, 437 (1994); A. Brignole, Phys. Lett. B **281**, 284 (1992); A. Dabelstein, Z. Phys. C **67**, 495 (1995); D. M. Pierce, J. A. Bagger, K. T. Matchev, and R. J. Zhang, Nucl. Phys. **B491**, 3 (1997).

[15] M. S. Carena, J. R. Espinosa, M. Quiros, and C. E. M. Wagner, Phys. Lett. B **355**, 209 (1995); M. S. Carena, M. Quiros, and C. E M. Wagner, Nucl. Phys. **B461**, 407 (1996); H. E. Haber, R. Hempfling, and A. H. Hoang, Z. Phys. C **75**, 539 (1997); J. R. Espinosa and I. Navarro, Nucl. Phys. **B615**, 82 (2001).

[16] R. Hempfling and A. H. Hoang, Phys. Lett. B **331**, 99 (1994).

[17] S. Heinemeyer, W. Hollik, and G. Weiglein, Phys. Rev. D **58**, 091701 (1998); Phys. Lett. B **440**, 296 (1998); R. J. Zhang, Phys. Lett. B **447**, 89 (1999); J. R. Espinosa and R. J. Zhang, J. High Energy Phys. 03 (2000) 026.

[18] S. Heinemeyer, W. Hollik, and G. Weiglein, Eur. Phys. J. C **9**, 343 (1999).

[19] J. R. Espinosa and R. J. Zhang, Nucl. Phys. **B586**, 3 (2000).

[20] G. Degrassi, P. Slavich, and F. Zwirner, Nucl. Phys. **B611**, 403 (2001).

[21] A. Brignole, G. Degrassi, P. Slavich, and F. Zwirner, Nucl. Phys. **B631**, 195 (2002).

[22] A. Brignole, G. Degrassi, P. Slavich, and F. Zwirner, Nucl. Phys. **B643**, 79 (2002); S. Heinemeyer, W. Hollik, H. Rzehak, and G. Weiglein, Eur. Phys. J. C **39**, 465 (2005).

[23] A. Dedes, G. Degrassi, and P. Slavich, Nucl. Phys. **B672**, 144 (2003).

[24] S. P. Martin, Phys. Rev. D **66**, 096001 (2002); **67**, 095012 (2003); **71**, 016012 (2005).

[25] S. P. Martin, Phys. Rev. D **75**, 055005 (2007); R. V. Harlander, P. Kant, L. Mihaila, and M. Steinhauser, Phys. Rev. Lett. **100**, 191602 (2008); **101**, 039901 (2008); P. Kant, R. V. Harlander, L. Mihaila, and M. Steinhauser, J. High Energy Phys. 08 (2010) 104.

[26] A. Pilaftsis, Phys. Rev. D **58**, 096010 (1998); Phys. Lett. B **435**, 88 (1998).

[27] D. A. Demir, Phys. Rev. D **60**, 055006 (1999); S. Y. Choi, M. Drees, and J. S. Lee, Phys. Lett. B **481**, 57 (2000); T. Ibrahim and P. Nath, Phys. Rev. D **63**, 035009 (2001); **66**, 015005 (2002).

[28] A. Pilaftsis and C. E. M. Wagner, Nucl. Phys. **B553**, 3 (1999); M. S. Carena, J. R. Ellis, A. Pilaftsis, and C. E. M. Wagner, Nucl. Phys. **B586**, 92 (2000); **B625**, 345 (2002).

[29] S. Heinemeyer, Eur. Phys. J. C **22**, 521 (2001).

[30] M. Frank, T. Hahn, S. Heinemeyer, W. Hollik, H. Rzehak, and G. Weiglein, J. High Energy Phys. 02 (2007) 047.

[31] S. Heinemeyer, W. Hollik, H. Rzehak, and G. Weiglein, Phys. Lett. B **652**, 300 (2007).

[32] S. Heinemeyer, W. Hollik, and G. Weiglein, Comput. Phys. Commun. **124**, 76 (2000); T. Hahn, W. Hollik, S. Heinemeyer, and G. Weiglein, in *Precision Higgs Masses with FeynHiggs 2.2*, eConf C050318, 0106 (2005); G. Degrassi, S. Heinemeyer, W. Hollik, P. Slavich, and G. Weiglein, Eur. Phys. J. C **28**, 133 (2003); T. Hahn, S. Heinemeyer, W. Hollik, H. Rzehak, and G. Weiglein, Comput. Phys. Commun. **180**, 1426 (2009).

[33] J. S. Lee, A. Pilaftsis, M. S. Carena, S. Y. Choi, M. Drees, J. R. Ellis, and C. E. M. Wagner, Comput. Phys. Commun. **156**, 283 (2004); J. S. Lee, M. Carena, J. Ellis, A. Pilaftsis, and C. E. M. Wagner, Comput. Phys. Commun. **180**, 312 (2009).

[34] B. C. Allanach, Comput. Phys. Commun. **143**, 305 (2002).

[35] A. Djouadi, J. L. Kneur, and G. Moultaka, Comput. Phys. Commun. **176**, 426 (2007).

[36] W. Porod, Comput. Phys. Commun. **153**, 275 (2003); W. Porod and F. Staub, arXiv:1104.1573.

[37] F. Staub, W. Porod and B. Herrmann, J. High Energy Phys. 10 (2010) 040.

[38] U. Ellwanger, Phys. Lett. B **303**, 271 (1993); T. Elliott, S. F. King, and P. L. White, Phys. Lett. B **305**, 71 (1993); **314**, 56 (1993); Phys. Rev. D **49**, 2435 (1994); P. N. Pandita, Z. Phys. C **59**, 575 (1993); Phys. Lett. B **318**, 338 (1993).

[39] U. Ellwanger and C. Hugonie, Phys. Lett. B **623**, 93 (2005).

[40] U. Ellwanger, J. F. Gunion, and C. Hugonie, J. High Energy Phys. 02 (2005) 066; U. Ellwanger and C. Hugonie, Comput. Phys. Commun. **175**, 290 (2006); **177**, 399 (2007).

[41] G. Degrassi and P. Slavich, Nucl. Phys. **B825**, 119 (2010).

[42] D. J. Miller, R. Nevzorov, and P. M. Zerwas, Nucl. Phys. **B681**, 3 (2004).

[43] J. F. Gunion and H. E. Haber, Nucl. Phys. **B272**, 1 (1986); arXiv:hep-ph/9301205.

[44] A. Denner, Fortsch. Phys. **41**, 307 (1993).

[45] P. H. Chankowski, S. Pokorski, and J. Rosiek, Phys. Lett. B **286**, 307 (1992); Nucl. Phys. **B423**, 437 (1994); A. Dabelstein, Z. Phys. C **67**, 495 (1995); Nucl. Phys. **B456**, 25 (1995).

[46] J. Kublbeck, M. Bohm, and A. Denner, Comput. Phys. Commun. **60**, 165 (1990); T. Hahn, Comput. Phys. Commun. **140**, 418 (2001); T. Hahn and C. Schappacher, Comput. Phys. Commun. **143**, 54 (2002).

[47] F. Staub, arXiv:0806.0538; Comput. Phys. Commun. **181**, 1077 (2010); **182**, 808 (2011).

[48] T. Hahn and M. Perez-Victoria, Comput. Phys. Commun. **118**, 153 (1999); T. Hahn, Comput. Phys. Commun. **178**, 217 (2008).

[49] F. del Aguila, A. Culatti, R. Munoz Tapia, and M. Perez-Victoria, Nucl. Phys. **B537**, 561 (1999).

[50] T. Hahn and M. Perez-Victoria, Comput. Phys. Commun. **118**, 153 (1999).

[51] W. Siegel, Phys. Lett. B **84**, 193 (1979); D. M. Capper, D. R. T. Jones, and P. van Nieuwenhuizen, Nucl. Phys. **B167**, 479 (1980).

[52] P. Z. Skands, B. C. Allanach, H. Baer, C. Balazs, G. Belanger, F. Boudjema, A. Djouadi, and R. Godbole *et al.*, J. High Energy Phys. 07 (2004) 036; B. C. Allanach, C. Balazs, G. Belanger, M. Bernhardt, F. Boudjema, D. Choudhury, K. Desch, and U. Ellwanger *et al.*, Comput. Phys. Commun. **180**, 8 (2009); F. Mahmoudi, S. Heinemeyer, A. Arbey, A. Bharucha, T. Goto, T. Hahn, U. Haisch, and S. Kraml *et al.*, Comput. Phys. Commun. **183**, 285 (2012).

[53] K. Nakamura *et al.* (Particle Data Group), J. Phys. G **37**, 075021 (2010) and 2011 partial update for the 2012 edition.

[54] R. Barate *et al.* (LEP Working Group for Higgs boson searches), Phys. Lett. B **565**, 61 (2003); S. Schael *et al.* (ALEPH and DELPHI, L3, and OPAL Collaborations), Eur. Phys. J. C **47**, 547 (2006).

[55] The TEVNPH Working Group for the CDF and D0 Collaborations, Report No. FERMILAB-PUB-09-394-E, CDF Note 9888, D0 Note 5980-CONF.

[56] ATLAS Collaboration, Report No. ATLAS-CONF-2011-135; G. Aad *et al.* (ATLAS Collaboration), Phys. Lett. B **705**, 435 (2011); ATLAS Collaboration, Phys. Rev. Lett. **107**, 231801 (2011); ATLAS Collaboration, Phys. Rev. Lett. **107**, 221802 (2011); ATLAS Collaboration, Phys. Lett. B **705**, 452 (2011); G. Aad *et al.* (ATLAS Collaboration), Phys. Lett. B **707**, 27 (2012); K. Sung (f. t. C. Collaboration), arXiv:1109.2457; C. Charlot (f. t. C. collaboration), arXiv:0906.1666; CMS Collaboration, notes CMS-PAS-HIG-11-020,-021,-022,-012,-013,-014,-015,-016 and -017.

[57] ATLAS Collaboration, Report No. ATLAS-CONF-2011-157; CMS Collaboration, Report No. CMS-PAS-HIG-11-023.

[58] P. Bechtle, O. Brein, S. Heinemeyer, G. Weiglein, and K. E. Williams, Comput. Phys. Commun. **181**, 138 (2010); **182**, 2605 (2011).

[59] S. Chatrchyan *et al.* (CMS Collaboration), Phys. Rev. Lett. **107**, 221804 (2011); G. Aad *et al.* (ATLAS Collaboration), arXiv:1109.6572.